Science of the Total Environment 955 (2024) 177080

Contents lists available at ScienceDirect

Science of the Total Environment

journal homepage: www.elsevier.com/locate/scitotenv

Impact of emerging pollutants mixtures on marine and brackish phytoplankton: diatom *Phaeodactylum tricornutum* and cyanobacterium *Microcystis aeruginosa*

Lilianna Sharma [a,*], Błażej Kudłak [b], Joanna Stoń-Egiert [a], Grzegorz Siedlewicz [a], Ksenia Pazdro [a]

[a] Institute of Oceanology, Polish Academy of Sciences, Powstańców Warszawy 55, 81-712 Sopot, Poland
[b] Department of Analytical Chemistry, Faculty of Chemistry, Gdańsk University of Technology, 11/12 Narutowicza Str., 80-233 Gdańsk, Poland

HIGHLIGHTS

- Target microorganisms sensitive to the presence of low levels of studied analytes
- Pigment composition of studied micro-organisms strongly affected by target analytes
- High sensitivity of phycobiliproteins as stress response markers in *M. aeruginosa*
- Chlorophyll *a* fluorescence parameter changes indicating stress defense mechanisms
- Presence of antagonistic interactions within most of the binary mixtures

GRAPHICAL ABSTRACT

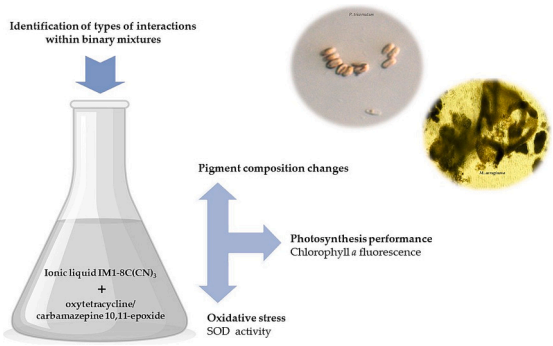

ARTICLE INFO

Editor: Damià Barceló

Keywords:
Mixture effects
Ionic liquids
Pharmaceuticals
Marine environment
Phytoplankton pigments

ABSTRACT

Pharmaceuticals and ionic liquids (ILs) are emerging as significant micropollutants with environmental presence and potential ecological impacts. The possible simultaneous occurrence of these two groups of pollutants in aquatic environments raises complex challenges due to their diverse chemical properties and potential for interactive effects. Given the documented widespread presence of pharmaceuticals and the emerging concerns about ILs, the study aims to evaluate the adverse effects of binary mixtures of imidazolium ionic liquid IM1-8C $(CN)_3$ and two representatives of pharmaceuticals: antibiotic oxytetracycline (OXTC) and metabolite carbamazepine 10,11 epoxide (CBZ-E) on the brackish cyanobacterium *Microcystis aeruginosa* and the marine diatom *Phaeodactylum tricornutum* during chronic exposure experiments. A comprehensive approach was employed, incorporating various endpoints including oxidative stress, chlorophyll *a* fluorescence, detailed photoprotective and photosynthetic pigment profiles of target microorganisms to assess modes of action and identify the mixture effects of the selected substances.

The observed alterations in pigment production affecting carotenoids synthesis in both selected species may be attributed to the differential impacts of these substances on the photosynthetic pathways and metabolic processes in the cyanobacterial and diatom cells. Changes in chlorophyll *a* fluorescence-specific parameters suggest impairment of the photosynthetic activity, particularly affecting the efficiency of photosystem II.

* Corresponding author.
E-mail address: lsharma@iopan.pl (L. Sharma).

https://doi.org/10.1016/j.scitotenv.2024.177080
Received 9 September 2024; Received in revised form 15 October 2024; Accepted 18 October 2024
Available online 29 October 2024

The application of Concentration Addition (CA) and Independent Action (IA) mathematical models, complemented by the evaluation of Model Deviation Ratios (MDR), revealed predominantly antagonistic interactions within the studied mixtures. The findings of this study provide important insights into the effects of mixtures of organic micropollutants and their potential impact on environment including brackish and marine waters.

1. Introduction

Micropollutants are defined as predominantly anthropogenic substances present in the environment at concentrations below 1 μg/l that are potentially toxic to living organisms. Examples of such substances include surfactants, personal care products, and active pharmaceutical compounds (Barbosa et al., 2016). The presence of micropollutants in the aquatic environment and their potential impact on freshwater microorganisms have been the subject of research for many years. However, the majority of studies has focused on assessing the risks associated with individual substances, often neglecting the combined effects of contaminant mixtures. Additionally, most existing data pertains to freshwater organisms and ecosystems, with marine environments frequently overlooked, despite being a significant sink for micropollutants (Hajji and Lucas, 2024; Sharma et al., 2021). Organisms are often simultaneously exposed to multiple chemicals, originating from various sources such as sewage waste, surface flows, and accidental spills. This leads to simultaneous and sequential exposure to chemical mixtures. Hence, it is crucial to incorporate the effects of mixtures in progressive risk assessment (Hayes et al., 2019; Drakvik et al., 2020). Assessing the effects of mixtures presents considerable challenges due to the vast number of possible combinations, the selection of appropriate compounds, concentration and the duration of exposure to these substances. Furthermore, there is limited information available regarding the toxicity of most chemicals already present in the environment. Additionally, novel chemicals are constantly being produced and introduced into the market each year.

Ionic liquids (ILs) stand out among emerging contaminants, constituting a diverse array of salts composed of both cations and anions (Oskarsson and Wright, 2019). According to the proposed classification by the German Federal Environmental Agency (Neumann and Schliebner, 2019), ionic liquids can be considered as persistent (P) and mobile (M), or even as very persistent (vP) and very mobile (vM) compounds. They are characterized by low melting points, often below room temperature, and can remain in a liquid state over a wide temperature range. Ionic liquids offer tailored thermophysical properties, prompting extensive research on their potential applications across various industrial sectors (Kaur et al., 2022). ILs can enter the environment through industrial processes, consumer products, laboratory use, landfills, and wastewater treatment plants. They are used in various applications and can be released into the environment through spills, disposal, or leaching. Imidazolium, pyridinium, and ammonium salts are among the most commonly utilized cations (Bubalo et al., 2014; Qureshi et al., 2014). In the past, there was an assumption that ionic liquids could persist as pollutants in aquatic environments. Nevertheless, recent studies have provided insights into their actual presence in both aquatic and terrestrial settings typically at concentrations ranging from nano to micrograms *per* liter (Probert et al., 2018; Leitch et al., 2020, 2021; Neuwald et al., 2021).

The toxicity of individual ionic liquids towards green algae and cyanobacteria has been previously investigated, revealing varying degrees of harmful effects depending on the ionic liquid's structure and concentration (Ghanem et al., 2015; Sydow et al., 2018; Chen et al., 2019; Fan et al., 2019a; Fan et al., 2019b; Jin et al., 2019; Cho et al., 2021). However, there remains a significant lack of information concerning the interactions between ionic liquids and other organic micropollutants present in the aquatic environment. Given this knowledge gap, determining the eventual potentiation of toxicity of ionic liquids in the presence of other xenobiotics is essential for conducting a proactive risk assessment. Pharmaceutical residues are widely detected across diverse aquatic environments, where they have been shown to exert detrimental effects on microbial communities. These contaminants, often originating from improper disposal and agricultural runoff, pose a significant threat to the ecological balance of aquatic systems. The polarity of these compounds plays a crucial role in their environmental behavior, influencing their widespread dispersion, high persistence, and bioavailability in aquatic ecosystems (Pinto et al., 2022). Coastal areas are widely recognized as highly sensitive environments, while marine regions are commonly regarded as potential reservoirs and sinks for micropollutants, as indicated by several studies (Moreno-González et al., 2014, 2015; Spindola et al., 2022). Therefore, the primary objective of this study is to address the existing gap by identifying and exploring the potential interactions involving binary mixtures of imidazolium-based IM1-8C$(CN)_3$ ionic liquid and other widely distributed organic pollutants present in aquatic compartments, specifically the antibiotic oxytetracycline (OXTC) and a transformation product of carbamazepine-metabolite carbamazepine 10,11-epoxide (CBZ-E) (Langford and Thomas, 2011; Björlenius et al., 2018; Siedlewicz et al., 2018). Consequently, the objective of this study is to evaluate the response of specific microorganisms, namely the freshwater cyanobacterium *Microcystis aeruginosa* inhabiting the brackish coastal waters of the Baltic Sea, and the marine diatom *Phaeodactylum tricornutum* present in the open water sea basin (Wasmund et al., 2016), to exposure to selected micropollutants. Given their rapid response times and high sensitivity to environmental stressors, algae are routinely used as indicator organisms in risk assessment studies. Due to their vulnerability to xenobiotics, cyanobacteria are among the primary test species in environmental risk assessment protocols (OECD, 2011). The selection of test organisms in this study is based on their relevance as established model organisms and their role in primary production and nutrient cycling within the Baltic Sea, a unique brackish ecosystem (Russo et al., 2023). Baltic Sea is particularly vulnerable to xenobiotic pollution due to its limited water exchange, low biodiversity, and relatively extensive catchment area. Furthermore, the region faces multiple anthropogenic pressures, including intensive agriculture, industrial activities, and dense coastal populations.

The assessment of microorganisms' responses is based on oxidative stress indicators, encompassing superoxide dismutase (SOD) activity, photosynthesis efficiency reflected in chlorophyll *a* fluorescence, as well as pigment concentrations, including chlorophylls and xanthophylls and phycobilins. Despite numerous studies attempting to depict synergistic or antagonistic interactions between the described chemicals and their combined effects on microorganisms, no research has employed a more sophisticated approach, such as the one used in this study. Concentration addition (CA) and independent action (IA) mathematical models predict the toxicity of mixtures composed of target substances characterized by either similar or distinct modes of action, respectively. In order to identify the type of interactions within the mixtures, the model deviation ratio (MDR) values were calculated verifying observations that single chemical-toxicological effect studies are insufficient in environmental hazard predictions.

2. Materials and methods

2.1. Chemicals

Ionic liquid standard 1-octyl-3-methylimidazolium tricyanomethide (IM1-8C$(CN)_3$, ≥97 %) was purchased from Iolitec (Germany).

Oxytetracycline hydrochloride (>99.9 %) (CAS no 2058-46-0), carbamazepine 10,11-epoxide (CAS no 36507-30-9) analytical standards, ethylenediaminetetraacetic acid disodium salt dihydrate (99.0–101.0 %) and tris(hydroxymethyl) aminomethane, sodium deoxycholate (CAS no 302-95-4), trichloroacetic acid (CAS no 76-03-9) ACS reagents, <99.8 %, were obtained from Sigma Aldrich/Merck KGaA (Darmstadt, Germany). Fresh standard solutions of the analyzed substances were prepared in Milli-Q water before commencing the experiments. Milli-Q water was acquired using the Milli-Q® Type 1 Ultrapure Water System (Merck KGaA, Darmstadt, Germany).

2.2. Determination of analytes concentration

In this current study, an evaluation was undertaken to validate and ensure the stability of target analytes independently throughout the entire experimental duration. The stability of OXTC under the given experimental conditions was previously affirmed by Siedlewicz et al. (2020). Given the consistency in the experimental parameters, it was deemed appropriate to refer to the previously acquired data. The UHPLC system coupled to a mass spectrometer (LC-MS-8050) with an electrospray ionization (ESI) source (Shimadzu, Japan) was utilized to verify the nominal versus measured concentration of IM1-8C$(CN)_3$. Comprehensive information on the method of determination of IL can be found in the descriptions provided by Maculewicz et al. (2022, 2023a, 2023b). The stability of the ionic liquid was independently confirmed, revealing a concentration decrease to half of the nominal value at the start of the experiment and maintained consistently lower level throughout the study to the final days of the experiments for both *M. aeruginosa* and *P. tricornutum*. Additionally, LC-MS analysis (following extraction on BAKERBOND Speedisk (H2O-Philic DVB) (JT Baker, Heidelberg, Germany)) revealed the stability of CBZ-E under the experimental conditions for both cyanobacterium and diatom.

2.3. Monocultures of algae and cyanobacteria

The targeted microorganisms included two species 1) *M. aeruginosa* PCC-7820, a freshwater cyanobacterium known for forming blooms and present in the brackish coastal waters of the Baltic Sea (the strain was acquired from the Pasteur Institute in France) and 2) *P. tricornutum* SAG 1090-1a, a model diatom present in the open waters of the Baltic Sea basin (obtained from the Algae Culture Collection at the University of Göttingen in Germany). The cultures of these species are accessible in the Microalgae and Bacteria Culture Collection at the Biochemistry Laboratory of the Institute of Oceanology Polish Academy of Sciences. Batch cultures of these species were raised in flasks containing liquid medium (616 and f/2 medium with 7 PSU artificial seawater used for *M. aeruginosa* and *P. tricornutum*, respectively, at a constant temperature of 22 ± 1 °C and a light intensity of 15 and 80 μmol photons m^{-2} s^{-1}, respectively). The cultures were harvested during the logarithmic growth phase and used as inoculants. The initial optical densities (OD) of *M. aeruginosa* and *P. tricornutum* were measured at a wavelength of 680 nm and found to be 0.59 and 0.06, respectively. The growth media were prepared following protocols described by Lyman and Fleming (1940) and Guillard (1975).

2.4. Experimental design

The experiment was divided into two separate phases (Fig. 1). The first phase focused on evaluation of effect of individual target analytes on growth and photosynthetic activity of the microorganisms aimed at obtaining half median effective concentration (EC_{50}) for each compound. In the second phase, the investigation revolved around examining the effects of three different concentrations of individual analytes and their binary mixtures. This evaluation was based on the analysis of chlorophyll *a* fluorescence, growth changes, pigment composition, and oxidative stress. The mixture treatment involved adding one of three concentration levels, namely C_1, C_2, and C_3, of the first target compound referred as substance 1 (S_1) to the second compound (S_2) for each analyte being tested. The EC_{50} of the given compounds corresponds to a 50 % inhibition of the photosynthetic activity of the selected microorganism (based on the value of F_v/F_m parameter), and it is represented by the C_3 value. The C_2 and C_1 values correspond to a reduction in the C_3 concentration by 33 % and 66 %, respectively. According to the European Chemicals Agency (ECHA, 2008) classification, toxicity categories and their corresponding EC_{50} concentration ranges are as follows: very toxic (EC_{50} values between 0.1 and 1 mg/l), slightly toxic (1–10 mg/l), moderately toxic (10–100 mg/l), and harmless (100–1000 mg/l). The EC_{50} values for carbamazepine 10,11-epoxide in the case of both target species were estimated to significantly exceed the >100 mg/l cutoff value. Therefore, three concentrations were proposed for the mixture treatments ($C_1 = 0.01$, $C_2 = 0.1$, and $C_3 = 1$ mg/l). The EC_{50} values were determined as 0.98 mg/l and 1.5 mg/l for oxytetracycline, and 0.1 mg/l and 8.0 mg/l for the ionic liquid, for *M. aeruginosa* and *P. tricornutum*, respectively. Table 1 presents the comprehensive list of target substances along with their corresponding applied concentrations and EC_{50} values. The individual effects of all C_1, C_2, and C_3 concentrations were investigated simultaneously. Prior to analysis, standard stock solutions of selected compounds were prepared in Milli-Q water. These target

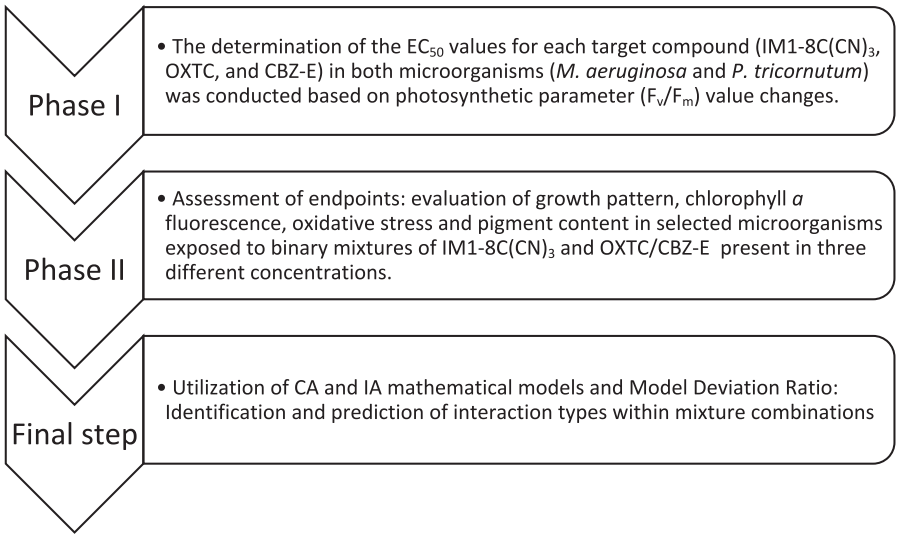

Fig. 1. Schematic presentation of experiment design.

analytes were then added to flasks containing the chosen algal or cyanobacterial monocultures, following the schematic presentation of the binary mixtures presented in Table S1. The total volume of the medium in each flask was 50 ml, with the initial optical density (OD) set at 0.06 (λ = 680 nm) for both target species. The initial number of cells for *P. tricornutum* (4.5×10^8 cells/ml) was identified by applying a Brüker chamber under a light microscope. The experiments were conducted over a period of 11 days, with optical density, chlorophyll *a* measurements, and subsample collections performed at the start of the experiment, on days 2, 5, 7, 9, and on the final 11th day. Optical density measurements were conducted using the HITACHI U-2800 UV-VIS spectrophotometer at wavelengths of 680 nm and 750 nm to evaluate growth pattern changes.

2.5. Pigment content

After an exposure time of 11 days, samples of algal and cyanobacterial cultures were collected using GF/F glass fibre filters and subsequently preserved at a temperature of −80 °C to facilitate further chromatographic analysis. The xanthophyll and chlorophyll pigments were extracted using an aqueous acetone solution (90 % *v*/v) through mechanical grinding and sonication. The resulting solution was then incubated in the absence of light at a temperature of 4 °C for a period of 2 h. Qualitative and quantitative analyses of the pigments were conducted using the Agilent HP1200 chromatographic system (Perlan Technologies, USA) with a C18 LichroCART™LiChrospher™ 100RP18e analytical column (250 × 4 mm; 5 μm (particle size); 100 Å (pore size) (Merck, Germany)) equipped with fluorescence and diode array absorbance detectors. The methodology employed in this analysis has been described in detail by Stoń-Egiert and Kosakowska (2005). Phycobilin extraction was performed with 10 mM hydrated disodium ethylenediaminetetraacetic acid (EDTA), 0.25 M Trizma Base, and 2 mg ml^{-3} lysozyme combined in a medium of final pH 5.5. The concentration of phycobiliproteins was determined spectrofluorometrically (Cary Eclipse, Agilent Technologies) following the methodology outlined by Sobiechowska-Sasim et al. (2014).

2.6. Oxidative stress

Upon the end of the experiment, the spectrophotometric measurement of the activities of representative antioxidant, total superoxide dismutase [SOD] in *M. aeruginosa* and *P. tricornutum* was carried out using commercially available kit (Elabscience Biotechnology Inc., China) in accordance with the manufacturer's instructions. The total superoxide dismutase detection was based on WST-1method, where 1 activity unit (U) was equivalent to a 50 % SOD inhibition ratio in the reaction system. The method had a sensitivity of 0.2 U/ml and a detection range of 0.2–14.4 U/ml. Samples for protein quantification were prepared using a modified trichloroacetic acid (TCA) precipitation method, as outlined by Peterson (1977, 1983) and Clayton et al. (1988). At the onset, cells collected on filters were homogenized in M NaOH. Following extraction (0.5 h), the samples underwent centrifugation to remove residual cellular and filter debris. The soluble proteins in the supernatant were precipitated using 3 ml of TCA (22 % *w/v* H_2O) and 0.6 ml of deoxycholate (DOC, 0.15 % w/v H_2O). The residue was resuspended in 0.1 M NaOH, and protein content in subsamples was determined using Bradford method (Bradford, 1976). Absorbance readings were taken at λ = 595 nm using a Thermo Scientific™ Varioskan microplate reader. Protein content was estimated by comparison with a standard bovine serum albumin (BSA) curve. Notably, the protein data obtained represent only the soluble protein fraction.

Table 1
The list of concentrations applied in the binary mixtures and the corresponding microorganisms.

Microorganism	Substance studied and its concentration (C_1, C_2 and C_3 in mg/l)			
		IM1-8C(CN)$_3$ (S_1)	OXTC (S_2)	CBZ-E (S_3)
M. aeruginosa	C_1	0.033	0.32	0.01
	C_2	0.066	0.64	0.10
	C_3 (EC_{50})	0.10	0.98	1.00[a]
P. tricornutum	C_1	2.64	0.49	0.01
	C_2	5.28	0.99	0.10
	C_3 (EC_{50})	8.00	1.50	1.00[a]

[a] EC_{50} value >100 mg/l.

2.7. The chlorophyll a fluorescence

The determination of chlorophyll *a* fluorescence emission transient (O-J-I-P transient) enables the analysis of different fluorescence parameters involving minimal (F_0) and maximal (F_m) fluorescence when all reaction centers are open (t = 0) and closed, respectively. It also includes variable fluorescence at a given time t (F_v) along with specific energy fluxes per reaction center (RC) including light absorption (ABS/RC), trapped and dissipated energy (TR0/RC, DI0/RC respectively) and electron transport (ET0/RC) (Strasser et al., 2004; Roháček et al., 2008). The parameter corresponding to the maximum quantum efficiency of the photosystem II (PSII) equal to the ratio of F_v/F_m, directly reflects photosynthesis performance and inhibition. All measurements of photosynthetic activity were conducted on dark-adapted algal samples in polystyrene cuvettes (volume 4 cm^3, optical length 1 cm) during the experiment (at the beginning, after 2, 4, 7, 9 days, and at the end of the experiment), using the AquaPen AP110-C fluorometer equipped with red (630 nm) and blue (455 nm) LED emitters, in accordance with the manufacturer's instructions (Photon Systems Instruments PSI, Czech Republic).

2.8. Mixture toxicity modeling

Both Concentration Addiction (CA) and Independent Action (IA) are established mathematical models commonly utilized in environmental risk assessment (Bliss, 1939; Plackett and Hewlett, 1952; Backhaus et al., 2000). These models assume an absence of interactions between the components, including no interference with distribution, uptake, or metabolism (Backhaus, 2014). The accuracy of each model was evaluated using the Model Deviation Ratio (MDR) approach, as demonstrated by Wieczerzak et al. (2016a). The MDR value of 1 signifies optimal compliance between the predicted and observed toxicity of a given mixture. Conversely, MDR values ranging from 0.50 to 0.71 indicate underestimation of mixture toxicity, implying higher toxicity than anticipated by either the CA or IA model. A MDR value of 1.40 to 2.00, on the other hand, suggests overestimation of mixture toxicity, indicating lower toxicity than predicted by either model. MDR values exceeding 2.0 denote antagonistic interactions among the mixture components. Conversely, values <0.5 indicate the presence of synergistic interactions (Wieczerzak et al., 2016a, 2016b). The calculation of MDR allowed for the comparison of predicted effects from IA and CA models to the observed effects under presumed experimental settings. MDR provides a quantitative measure of how well the chosen model aligns with experimental data and assists in assessing the type of interactions among substances. Table S2 presents basic details of the CA and IA models employed in the current study.

2.9. Statistical analysis

The results are presented as the mean value ± standard deviation (SD) of three independent repetitions (n = 3). Statistical tools one-way ANOVA and Dunnett's multiple comparison post hoc test (Microsoft Excel software) were applied for identification of data statistical dependencies ($p < 0.05$).

3. Results

3.1. Growth changes

3.1.1. M. aeruginosa

The presence of individual ionic liquid and oxytetracycline (OXTC) resulted in a concentration-dependent inhibition of cyanobacterial growth, with up to 60 % growth inhibition compared to the control. The impact of their binary mixtures predominantly exhibited additive effects, leading to an 85 % growth inhibition in the mixture containing the highest concentrations of both compounds relative to the control. Conversely, the presence of CBZ-E individually had no discernible effect on microorganism growth. In binary mixtures of IM1-8C(CN)$_3$ and CBZ-E, the growth inhibition of *M. aeruginosa* was primarily attributed to the presence of the ionic liquid, while CBZ-E exhibited a limited impact.

3.1.2. P. tricornutum

Similarly, the presence of ionic liquid and oxytetracycline (OXTC) individually resulted in a concentration-dependent inhibition of diatom growth, leading to approximately a 50 % decline in growth as the highest concentrations of the compounds. In the case of binary mixtures of both substances, the growth inhibition was smaller compared to the individual effects, especially at the highest C_3 concentrations, suggesting antagonistic effects within the mixtures. However, in the case of CBZ-E, growth stimulation was observed by 43 %, 64 %, and 78 % with increasing CBZ-E content. The binary mixtures of C_2 and C_3 $_{IM1\text{-}8C(CN)3}$ resulted in a 90 % growth inhibition of the organism.

Table S3 presents the detailed results of growth changes based on OD measurements of target microorganisms exposed to individual compounds and their binary mixtures.

3.2. Pigment composition

3.2.1. M. aeruginosa

In Fig. 2, the relative pigment composition of *M. aeruginosa* is depicted as a percentage of the control (for specific values including statistically significant results, please see Table S4 and S5). The pigments, namely β-carotene (β-car) zeaxanthin (Zea), echinenone (Echi), aphanizophyll (Apha), chlorophyllide (chlide) and phycobilins (phycoerythrin (PE) and phycocyanin (PC)) have been normalized with respect to chlorophyll *a* (chl-*a*) concentration. Normalizing pigment content with respect to chlorophyll *a* concentration enables a more accurate comparison of the relative abundance of individual pigments across different experimental conditions, independent of variations in sample biomass. However, in certain experimental variants where there is a significant decline in chl-*a* content, this approach may artificially inflate the relative concentrations of other pigments. To mitigate the risk of data misinterpretation, absolute pigment concentrations, expressed in μg/dm^3, were also considered. Additionally, expressing pigment levels as a percentage of the control provide clearer insights into the organism's adaptive responses and alterations in its photosynthetic apparatus. Exposure of the cyanobacterium to both the medium (C_2) and highest levels (C_3) of IM1-8C(CN)$_3$ (S_1) resulted in a significant inhibition of pigment production with the exception of chlorophyllide and aphanizophyll. The chlorophyll *a* (chl-*a*) content decreased by 61 % in response to exposure to the C_3 concentration of IL (Table S4). Conversely, exposure to OXTC (S_2) (Fig. 2A) led to a considerable increase in relative pigment content at all three concentration levels, with echinenone showing a six fold increase and aphanizophyll and β-carotene exhibiting a threefold increase. However, a proportional decrease in all absolute pigment concentrations was observed. Consistent with absolute values, the increase in relative pigment content was directly correlated with the rising concentration of the antibiotic. Simultaneously, there was a reduction in chlorophyll *a* concentration, accompanied by an increase in its derivatives including chlorophyllide *a* particularly in response to C_1/C_2 $_{OXTC}$. Exposure to OXTC resulted in a decrease of chlorophyll *a* content by 50 %, 86 %, and 98 % correlating with an increasing antibiotic concentration.

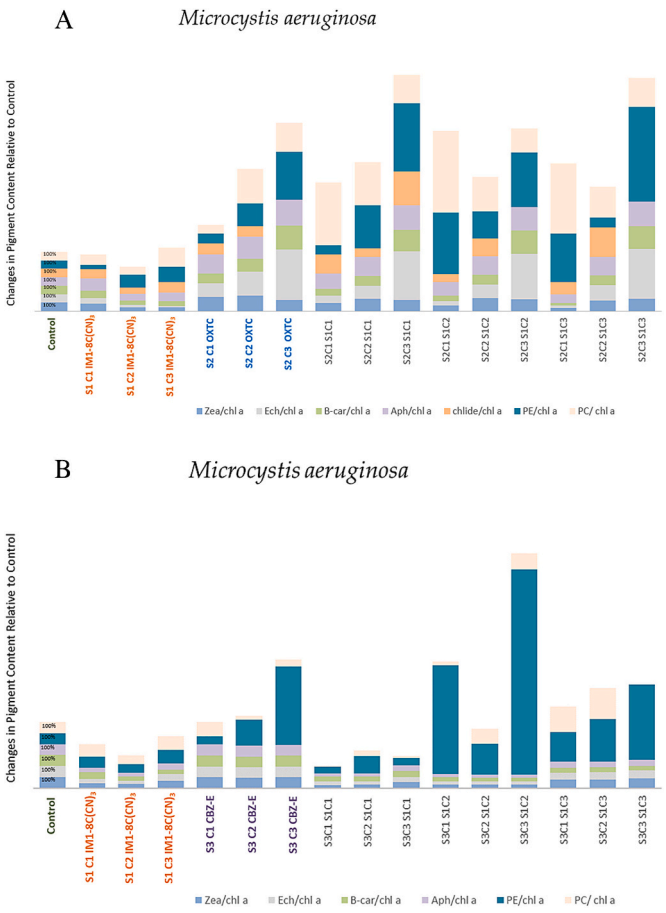

Fig. 2. Relative pigment content in *Microcystis aeruginosa* (the percentage changes in the relative contents of identified pigments, normalized to the concentration of chlorophyll *a* and presented as % of control) exposed to individual compounds and binary mixtures of IM1-8C(CN)$_3$ and OXTC (Fig. 2A) and carbamazepine 10,11-epoxide (Fig. 2B) after 11 days exposure time ($n = 3$). (S_1 IM1-8C(CN)$_3$ concentrations C_3 $_{IM1\text{-}8C(CN)3}$ = 0.1 mg/l, C_2 $_{IM1\text{-}8C(CN)3}$ = 0.066 mg/l, C_1 $_{IM1\text{-}8C(CN)3}$ = 0.033 mg/l, S_2 OXTC C_3 $_{OXTC}$ = 0.98, C_2 $_{OXTC}$ = 0.64 mg/l and C_1 $_{OXTC}$ = 0.32 mg/l, S_3 CBZ-E C_1 $_{CBZ\text{-}E}$ = 0.01, C_2 $_{CBZ\text{-}E}$ = 0.1, and C_3 $_{CBZ\text{-}E}$ = 1 mg/l).

In mixture treatments, a consistent reduction in absolute pigment concentrations was observed across all experimental variations, with a particularly notable decrease in chlorophyll *a* content. Binary mixtures containing C_2 and C_3 OXTC exhibited a pronounced suppressive effect on chlorophyll *a* levels compared to the control (Table S4). A decrease in the relative concentrations of zeaxanthin, echinenone, and β-carotene was identified in two specific combinations: the highest and medium concentrations of the ionic liquid combined with the lowest level of OXTC (Fig. 2A). Conversely, other mixture variations demonstrated relative increases in pigment content. Overall, all binary mixtures significantly altered the aphanizophyll/chl-*a* ratio, resulting in relative values increasing by over twofold. Additionally, a significant increase in the relative content of β-carotene was observed in response to mixtures containing the highest OXTC concentration.

Exposure of *M. aeruginosa* to the single compound CBZ-E (S_3) did not produce statistically significant changes in the relative pigment ratios (Fig. 2B). However, the combination of C_1 $_{CBZ\text{-}E}$ and C_1 $_{IM1\text{-}8C(CN)3}$ resulted in a statistically significant 30 % increase in chlorophyll *a* content (Table S4). Conversely, only those mixtures containing the highest concentration of the ionic liquid (IL) led to a significant reduction in chlorophyll *a* levels, with a decrease of 75 %. Binary mixtures

containing intermediate concentrations of IM1-8C(CN)$_3$ caused a nearly 70 % reduction in pigment-to-chlorophyll *a* ratios, affecting β-carotene (β-car/chl *a*), zeaxanthin (Zea/chl *a*), echinenone (Echi/chl *a*), and aphanizophyll (Apha/chl *a*). Specifically, the relative levels of β-carotene and aphanizophyll decreased by approximately 60 % and 50 %, respectively, in the presence of mixtures containing $C_{3\ IM1\text{-}8C(CN)3}$. These observed variations in pigment levels were directly correlated with the concentration of the ionic liquid. Notably, chlorophyllide *a* pigment was detected in all binary mixtures, including those with the highest concentration of IL.

Phycobiliproteins are a group of water-soluble pigments primarily found in cyanobacteria and certain eukaryotic algae. Fig. S1. presents the relative pigment composition of ***M. aeruginosa*** as a percentage of the control (for specific values and statistically significant results, please see Table S5). The phycobiliproteins content has been normalized with respect to chlorophyll *a*. The rise in phycobiliproteins concentration exhibits a direct proportionality to the increasing levels of both ionic liquid and antibiotic individually. In the context of combination treatments, noticeable increases, spanning several-fold, are apparent for both phycocyanin and phycoerythrin. An elevation exceeding tenfold is observed in the concentration of phycoerythrin in the case of the binary mixture of the highest concentrations (C_3) of both analytes.

Exposure to medium and highest concentrations of CBZ-E resulted in an increase in phycoerythrin level and a decrease in phycocyanin concentration, indicating the sensitivity of phycobiliproteins as stress response markers. In mixture treatments, there was a stimulation of phycoerythrin production, while phycocyanin significantly declined in all mixtures except for C_3 of IM1-8C(CN)$_3$ and C_1 and C_2 of CBZ-E. In the binary mixtures featuring the highest concentrations of both analytes, phycocyanin was absent. The observed trends are consistent when considering both relative or absolute pigment contents.

3.2.2. *P. tricornutum*

Fig. 3 portrays the relative pigment composition (ratios of fucoxanthin (fuco), violaxanthin (violax), diatoxanthin (diatox), diadinoxanthin (diad), β-carotene (β-car), chlorophyll *c*1 + c2, chlorophyllide *a* (chlide) to chlorophyll *a* concentration) of *P. tricornutum* upon exposure to IM1-8C(CN)$_3$, OXTC and CBZ-E present individually and in binary mixtures. The pigment composition is presented as a percentage relative to the control and normalized to the concentration of chlorophyll *a* (specific numerical values and statistically significant results are presented in Table S6). The increasing concentration of the ionic liquid led to a proportional decrease in the absolute content of all pigments, including an almost 70 % reduction in chlorophyll *a* concentration in response to $C_{3\ IM1\text{-}8C(CN)3}$. In terms of relative values, the lowest concentration of the ionic liquid resulted in approximately two-fold increase in the relative levels of β-carotene and diatoxanthin. At medium concentration, a substantial four-fold rise in diatoxanthin relative content was observed, along with a 2.5-fold increase in relative values of violaxanthin.

Furthermore, at the highest IL concentration, a 55 % surge in relative diatoxanthin content compared to the control is observed. The presence of OXTC resulted in slight decreases in the absolute concentrations of all pigments (Table S6). In terms of relative values (Fig. 3A), a twofold increase was observed in fucoxanthin and chlorophyllide *a* when exposed to $C_{3\ OXTC}$ along statistically significant increases in the relative content of diadinoxanthin and β-carotene. Conversely, when examining the antibiotic content at its highest concentration, diatoxanthin was found to be completely absent. In the mixture variants, a significant increase of nearly threefold was observed in relative diatoxanthin levels, except for the binary mixtures containing $C_{3\ OXTC}$ and $C_1/C_{2\ IM1\text{-}8C(CN)3}$ where this increase was absent. An approximately 50 % reduction in chlorophyll *a* content was noted in response to the exposure to $C_{3\ OXTC}$/$C1_{\ IM1\text{-}C(CN)3}$ and $C_{2\ IM1\text{-}C(CN)3}$ mixtures, as well as in binary mixtures with the highest concentration of both compounds. Simultaneously, an increase of the chlorophyll *a* derivatives, specifically chlorophyllide was observed. The mixture with the highest concentrations of both target

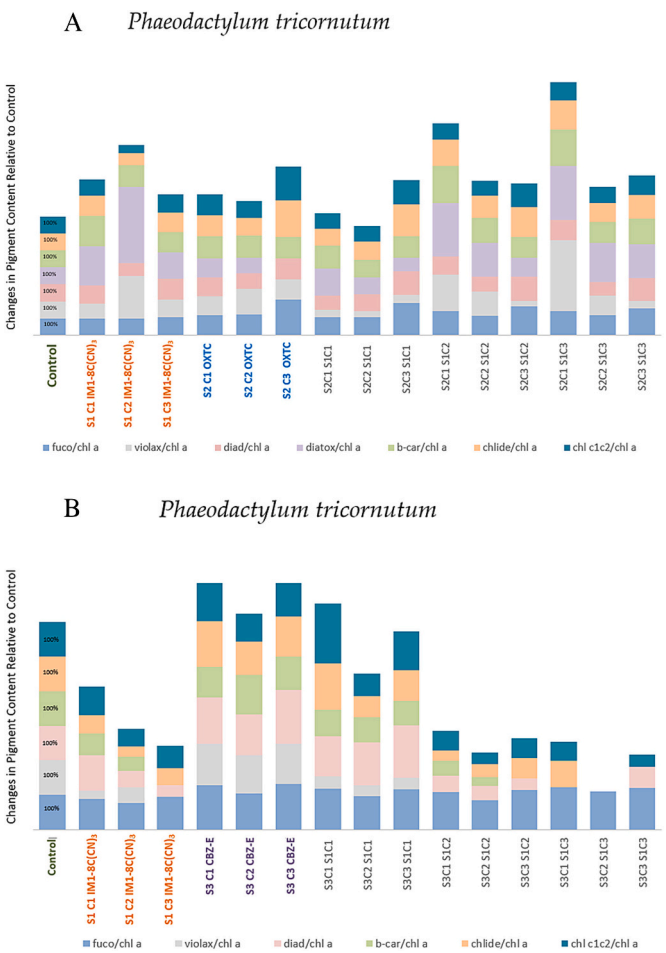

Fig. 3. Relative pigment content in *Phaeodactylum tricornutum* (the percentage changes in the relative contents of identified pigments, normalized to the concentration of chlorophyll *a* compared to control) exposed to binary mixtures of IM1-8C(CN)$_3$ (S_1) and OXTC (S_2) (A) and carbamazepine 10,11-epoxide (S_3) (B) after 11 days exposure time ($n = 3$). (IM1-8C(CN)$_3$ concentrations $C_{3\ IM1\text{-}8C(CN)3}$ = 8.0 mg/l, $C_{2\ IM1\text{-}8C(CN)3}$ = 5.28 mg/l, $C_{1\ IM1\text{-}8C(CN)3}$ = 2.64 mg/l, OXTC $C_{3\ OXTC}$ = 1.5 mg/l, $C_{2\ OXTC}$ = 0.99 mg/l and $C_{1\ OXTC}$ = 0.49 mg/l, CBZ-E $C_{1\ CBZ\text{-}E}$ = 0.01, $C_{2\ CBZ\text{-}E}$ = 0.1, and $C_{3\ CBZ\text{-}E}$ = 1 mg/l).

compounds resulted in the statistically significant increases of all pigments relative content, except for violaxanthin, which exhibited a 56 % relative decrease compared to control. The presence of CBZ-E (Fig. 3B) alone did not yield discernible effects on relative pigment ratios and chlorophyll *a* levels, except for diadinoxanthin, which exhibited a 31 %, 18 % and 56 % increase when exposed to $C_1/C_2/C_{3\ CBZ\text{-}E}$, respectively. However, when combined with the ionic liquid, notable reductions in all pigment concentrations, both absolute and relative, were observed. The most pronounced effects were evident at the highest analytes concentrations, resulting in cellular death. Diatoxanthin was detected in samples with medium and highest ionic liquid content, as well as in all mixture treatments except $C_{3\ IM1\text{-}8C(CN)3}$ and $C_1/C_{2\ CBZ\text{-}E}$.

3.3. Oxidative stress

Fig. 4 illustrates the total superoxide dismutase (T-SOD) activity normalized based on protein content (mg/ml), in both species exposed to single analytes and their binary mixtures. It is presented as a percentage relative to the control.

In cells of *M. aeruginosa* exposed to binary mixtures with medium and high levels of ionic liquid and OXTC/CBZ-E, up to twofold increase in T-SOD production was observed (Fig. 4A and B). A similar twofold

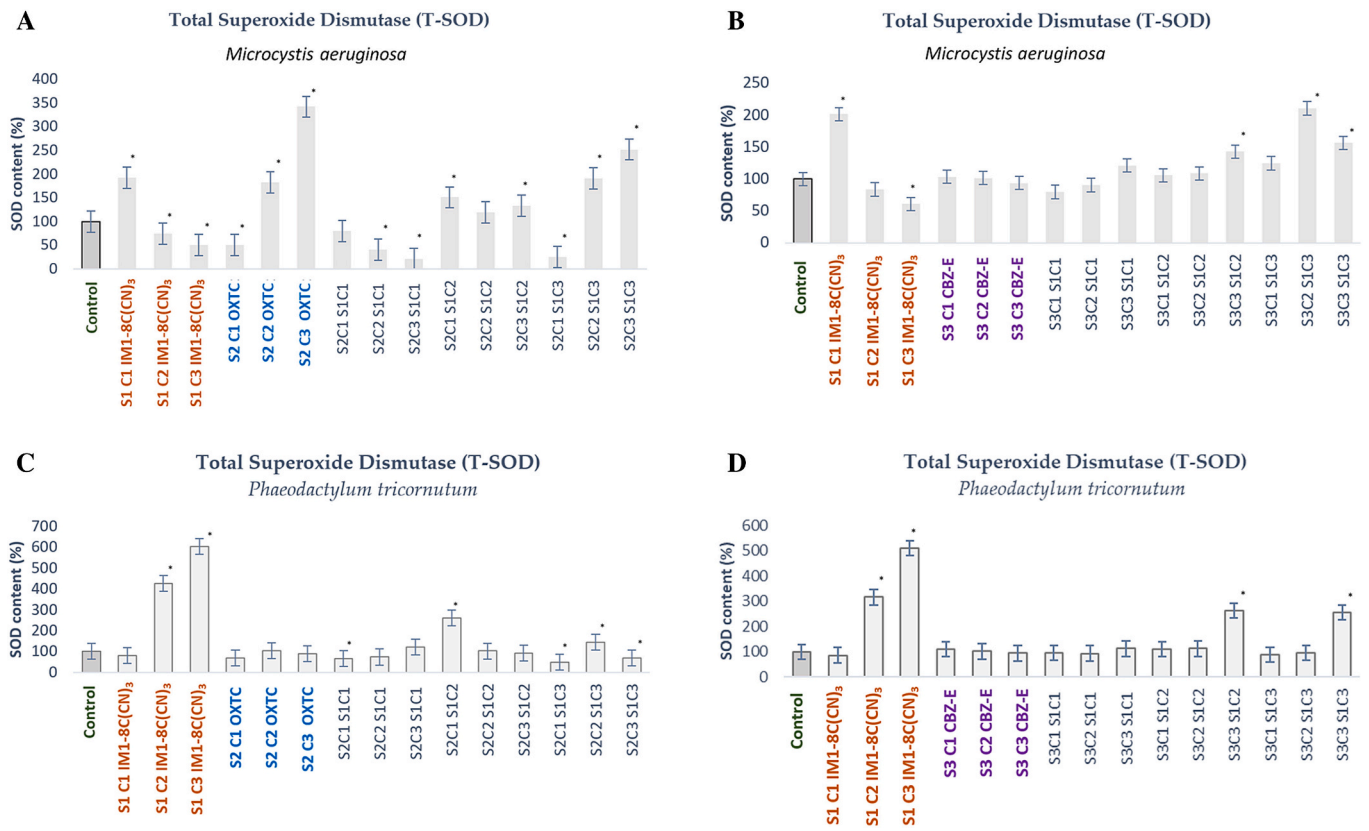

Fig. 4. Total Superoxide Dismutase (T-SOD) activity in *Microcystis aeruginosa* and *Phaeodactylum tricornutum* exposed to binary mixtures of IM1-8C(CN)$_3$ (S_1) and OXTC (S_2) (A) and carbamazepine 10,11-epoxide (S_3) (B), after an exposure period of 11 days ($n = 3$). The T-SOD activity is expressed as a percentage relative to the control, normalized based on protein content.

increase was also noted in response to the highest concentration of ionic liquid and a medium level of OXTC present individually. The highest concentration of antibiotic resulted in a threefold increase in relative T-SOD activity. A comparable trend was observed in cells of *P. tricornutum,* where exposure to medium and high levels of IM1-8C(CN)$_3$ led to over fivefold increases in T-SOD activity. The mixture of medium and high IL and C_3 CBZ-E concentrations resulted in over twofold increases (Fig. 4D), whereas the combination of highest concentrations of both ionic liquid and antibiotic led to 32 % of T-SOD activity (Fig. 4C).

3.4. The chlorophyll a fluorescence

3.4.1. M. aeruginosa

Fig. 5. presents the cumulative effect of the test substances expressed as a change in the value of the F_v/F_m parameter [%] (compared to the control (for specific values please see Table S7) where IM1-8C(CN)$_3$ (S_1), OXTC (S_2) and CBZ-E (S_3)). F_v/F_m is a measure of the maximum efficiency of PSII and is often used as an indicator of the overall health and stress level of photosynthetic organisms. F_v stands for variable fluorescence, which represents the difference between the maximum and minimum fluorescence levels, while F_m is the maximum fluorescence, the highest fluorescence level measured when all PSII reaction centers are closed (saturated with light). The individually applied concentrations of the ionic liquid and the highest level of OXTC resulted in significant inhibition of the F_v/F_m parameter, suggesting that the photosynthetic activity of cyanobacterial cells is impaired (Fig. 5A). The lower and medium values of the antibiotic resulted in stimulation. Exposure of *M. aeruginosa* to mixtures of the highest level of OXTC and to all three concentrations of ionic liquid resulted in a sharp decrease of the parameter. In all other cases, stimulation of photosynthetic activity can be observed. However, an opposite trend was noted with CBZ-E, where the F_v/F_m values remained stable when exposed to the single compound. In contrast, in the binary mixtures with $C_{3\ IM1\text{-}8C(CN)3}$ the toxicity of mixture significantly increases (Fig. 5B).

The ABS/RC parameter (Fig. S2/S3) provides information about the efficiency of light harvesting per active reaction center. The sharp increase in ABS/RC as a reaction to $C_{3\ IM1\text{-}8C(CN)3}$ and $C_{3\ OXTC}$ and their mixtures could be a compensatory mechanism employed by the microorganism to enhance light absorption. Under stress, the organism might attempt to capture more light energy to offset any negative impacts on its photosynthetic efficiency. The presence of CBZ-E individually or in the mixtures did not significantly influence the ABS/RC ratio values.

ET_0/RC serves as a measure of the efficiency of energy transfer per active reaction center, providing insights into the effectiveness of energy transfer within the photosynthetic system (Fig. S2/S3). In the context of $C_{3\ OXTC}$ and binary mixtures containing $C_{3\ OXTC}$, a pronounced reduction in ET_0/RC was noted. This decline in energy transfer efficiency and subsequent decrease in ET_0/RC may be attributed to impairments in electron transport and the occurrence of oxidative damage. The increase of the parameter could be observed in the case of exposition to CBZ-E and most of its mixture treatments. DI_0/RC reflects the density of active reaction centers per excited cross-section, providing insights into the arrangement of reaction centers. An increase of DI_0/RC was observed as a response to all target micropollutants and their binary mixtures. Microorganisms exposed to micropollutants may increase the synthesis of active reaction centers as a stress and compensatory response. This adaptive strategy could lead to a higher density of active reaction centers, contributing to the observed increase in DI_0/RC.

3.4.2. P. tricornutum

Fig. 6A. illustrates the impact of single compounds and the oxytetracycline and ionic liquid IM1-8C(CN)$_3$ mixtures on the PS II photosystem's

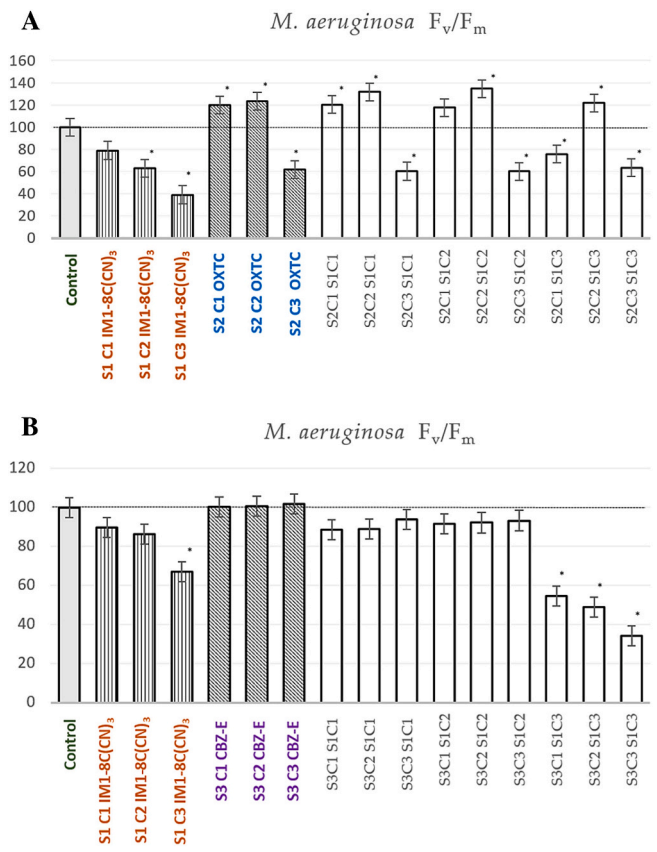

Fig. 5. The parameter F_v/F_m (the maximum quantum efficiency of PSII) values in *Microcystis aeruginosa* exposed to single compounds: IM1-8C(CN)$_3$ (S_1), oxytetracycline (S_2) (A) and carbamazepine 10,11-epoxide (S_3) (B) and their binary mixtures after 11 days exposure time ($n = 3$).

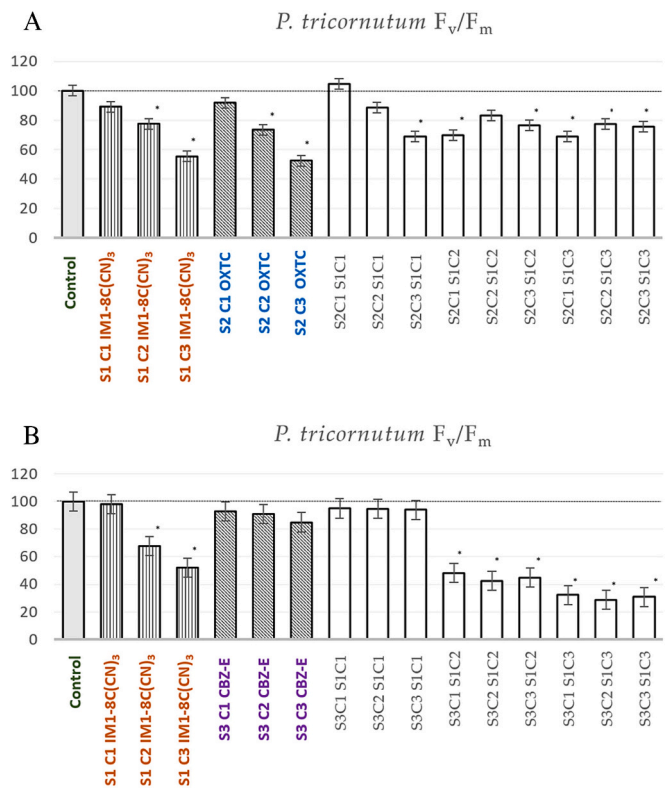

Fig. 6. The parameter F_v/F_m (the maximum quantum efficiency of PSII) values in *Phaeodactylum tricornutum* exposed to single compounds: IM1-8C(CN)$_3$ (S_1), oxytetracycline (S_2) (A) and carbamazepine 10,11-epoxide (S_3) (B) and their binary mixtures after 11 days exposure time (n = 3).

performance (F_v/F_m) in *P. tricornutum* (for specific values, please see Table S7). With the exception of mixture of $C_{1\ IM1\text{-}8C(CN)3}$ and $C_{1\ OXTC}/C_{2\ OXTC}$, all other binary mixtures exhibit an inhibition of photosynthetic efficiency. Notably, the presence of $C_{3\ IM1\text{-}8C(CN)3}$ and $C_{3\ OXTC}$ leads to a marked increase in ABS/RC and DI_0/RC ratios (Figs. S4 and S5), although this effect is less pronounced in the mixture variants. Mixtures containing $C_{3\ OXTC}$ display a significant rise in ET_0/RC, while the presence of C_1 and $C_{2\ OXTC}$ inhibits energy transfer. $C_{3\ CBZ\text{-}E}$ (Fig. 6B) leads to 15 % of inhibition of F_v/F_m compared to the control, while C_1 and C_2 have not influenced the parameter. However, in all mixture variants, except those containing $C_{1\ IM1\text{-}8C(CN)3}$ the photosynthetic efficiency (as indicated by F_v/F_m) in significantly reduced. An opposite trend is observed with the DI_0/RC parameter, where its value increases in response to the highest concentrations of CBZ-E individually, as well as in binary mixtures containing medium and high level of the ionic liquid. Additionally, all concentrations of CBZ-E result in relative decrease in ET_0/RC by 19 %, 24 % and 39 % compared to the control, respectively.

3.5. Concentration addition and independent action models

3.5.1. M. aeruginosa

3.5.1.1. Growth changes. According to the CA model (Table 2), growth change is significantly affected by the mixture of ionic liquid and OXTC at all studied concentrations, with a very strong indication of antagonism at the highest and mid-level content of OXTC. Importantly, the highest concentration of IMI-8C(CN)$_3$ and the lowest concentration of OXTC lead to synergistic response, confirming the serious threat posed by lower levels of this chemical. CBZ-E generally exhibits an antagonistic impact on IL toxicity at its highest concentration, particularly for the lowest and mid-level concentrations of IL. However, at the highest concentration of the ionic liquid, increasing concentrations of CBZ-E led the model to underestimate the effects of the mixture, which is notable from an environmental perspective, particularly in the case of accidental spills of the ionic liquid into environmental compartments. The IA model, in all cases, shows overestimation and an antagonistic impact of OXTC on ionic liquid, which is a surprising result but still in accordance with most observations from the CA model. The impact of CBZ-E on IMI-8(CN)$_3$ toxicity is clearly characterized by overestimation according to the IA model.

3.5.2. Photosynthetic activity

The CA model (Table 3) indicates that increasing concentrations of OXTC exhibit an ultrastrong antagonistic effect on the toxicity of IMI-8(CN)$_3$ at its lowest concentration. Conversely, the lowest concentration of OXTC demonstrates a strong synergistic effect in the mixture with IMI-8(CN)$_3$ as its concentration increases. The behavior of CBZ-E is similar to that of OXTC, although only one case of underestimation is observed, along with several antagonistic interactions. The IA model reflects interactions between IL and OXTC in a less precise manner, with three cases of overestimation at the highest content of OXTC, consistent with the trend presented by the CA model. For CBZ-E, an increasing content at C_3 of IMI-8(CN)$_3$ shows a clear trend from overestimation to antagonistic behavior.

3.5.3. P. tricornutum

3.5.3.1. Growth changes. The growth of diatoms (Table 4) is impacted by the IMI-8C(CN)$_3$-OXTC mixture in a manner similar to the effects observed on photosynthetic activity, showing a clear division of trends from underestimation to antagonism. CBZ-E affects IL toxicity antagonistically in almost all the mixtures studied. According to the IA model,

Table 2
The MDR values calculated based on growth changes (OD values) of *Microcystis aeruginosa* exposed to mixtures of S_1 – IM1-8C(CN)$_3$ and S_2-OXTC/S_3-CBZ-E for both CA and IA models. MDR values are interpreted as follows: values <0.5 indicate synergism, 0.5–0.7 reflect underestimation, 1.4–2.0 indicate overestimation, >2.0 suggest antagonism, and values between 0.71 and 1.4 show no significant trend.

Mixture of $S_{1\ IM1\text{-}8C(CN)3}$ and $S_{2\ OXTC}$						
	CA				**IA**	
	S_1C_1	**S_1C_2**	**S_1C_3**		**S_1C_1**	**S_1C_2**	**S_1C_3**
S_2C_1	1.299	0.692	0.475		1.559	1.560	1.508
S_2C_2	12.354	2.611	1.053		2.844	3.373	3.007
S_2C_3	164.615	7.384	2.796		5.542	5.682	4.488
Mixture of $S_{1\ (IM1\text{-}8C(CN)3}$ and $S_{3\ CBZ\text{-}E}$						
	S_1C_1	**S_1C_2**	**S_1C_3**		**S_1C_1**	**S_1C_2**	**S_1C_3**
S_3C_1	0.922	0.746	0.641		0.979	1.501	1.650
S_3C_2	5.386	1.383	0.685		1.025	1.514	1.618
S_3C_3	76.601	2.150	1.263		1.531	1.473	1.643

Table 3
The MDR values calculated based on photosynthetic activity changes (F_m/F_v parameter values) of *Microcystis aeruginosa* exposed to mixtures of S_1 – IM1-8C(CN)$_3$ and S_2-OXTC/S_3-CBZ-E for both CA and IA models. MDR values are interpreted as follows: values <0.5 indicate synergism, 0.5–0.7 reflect underestimation, 1.4–2.0 indicate overestimation, >2.0 suggest antagonism, and values between 0.71 and 1.4 show no significant trend.

Mixture of $S_{1\ IM1\text{-}8C(CN)3}$ and $S_{2\ OXTC}$						
	CA				**IA**	
	S_1C_1	**S_1C_2**	**S_1C_3**		**S_1C_1**	**S_1C_2**	**S_1C_3**
S_2C_1	0.577	0.292	0.319		0.765	0.731	1.015
S_2C_2	4.031	0.621	0.268		0.798	0.809	0.942
S_2C_3	79.863	1.912	0.926		1.730	1.785	1.765
Mixture of $S_{1\ (IM1\text{-}8C(CN)3}$ and $S_{3\ CBZ\text{-}E}$						
	S_1C_1	S_1C_2	S_1C_3		**S_1C_1**	**S_1C_2**	**S_1C_3**
S_3C_1	1.068	0.555	0.743		1.127	1.092	1.834
S_3C_2	5.889	1.008	0.904		1.126	1.087	2.047
S_3C_3	51.531	1.599	2.353		1.069	1.075	2.929

the highest content of OXTC shows an antagonistic impact on IMI-8C(CN)$_3$ toxicity. CBZ-E impacts the effect of IMI-8C(CN)$_3$ in an antagonistic manner, with two cases of overestimation confirmed.

3.5.3.2. Photosynthetic activity. The impact of OXTC on the ionic liquid is quite complex and requires further studies, as the levels of indispensability/toxicity are closely aligned in the given mixtures according to the CA model (Table 5). The toxicity of IMI-8(CN)$_3$ at its highest concentration may be impacted by OXTC in a synergistic manner, while at its lowest concentration (which is more plausible in environmental contexts), it exhibits an antagonistic interaction – a quite uncommon and interesting behavior. The trend line of CBZ-E's impact on ionic liquid toxicity follows that of OXTC, exhibiting predominantly antagonistic interactions, although synergistic behavior was not confirmed.

Table 4
The MDR values calculated based on growth changes (OD values) of *Phaeodactylum. tricornutum* exposed to mixtures of S_1 – IM1-8C(CN)$_3$ and S_2-OXTC/S_3-CBZ-E for both CA and IA models. MDR values are interpreted as follows: values <0.5 indicate synergism, 0.5–0.7 reflect underestimation, 1.4–2.0 indicate overestimation, >2.0 suggest antagonism, and values between 0.71 and 1.4 show no significant trend.

Mixture of $S_{1\ IM1\text{-}8C(CN)3}$ and $S_{2\ OXTC}$						
	CA			**IA**		
	S_1C_1	**S_1C_2**	**S_1C_3**	**S_1C_1**	**S_1C_2**	**S_1C_3**
S_2C_1	0.997	0.568	0.594	1.038	1.575	1.966
S_2C_2	5.734	1.019	0.768	1.112	1.538	2.296
S_2C_3	80.103	2.244	1.894	2.175	2.067	2.917
Mixture of $S_{1\ (IM1\text{-}8C(CN)3}$ and $S_{3\ CBZ\text{-}E}$						
	S_1C_1	**S_1C_2**	**S_1C_3**	**S_1C_1**	**S_1C_2**	**S_1C_3**
S_3C_1	0.853	2.789	2.337	1.129	6.973	7.426
S_3C_2	9.547	6.421	3.350	1.847	8.724	13.441
S_3C_3	91.193	11.733	5.505	1.920	12.772	12.698

Table 5
The MDR values calculated based on photosynthetic activity changes (F_m/F_v parameter values) of *Phaeodactylum tricornutum* exposed to mixtures of S_1 – IM1-8C(CN)$_3$ and S_2-OXTC/S_3-CBZ-E for both CA and IA models. MDR values are interpreted as follows: values <0.5 indicate synergism, 0.5–0.7 reflect underestimation, 1.4–2.0 indicate overestimation, >2.0 suggest antagonism, and values between 0.71 and 1.4 show no significant trend.

Mixture of $S_{1\ IM1\text{-}8C(CN)3}$ and $S_{2\ OXTC}$						
	CA			**IA**		
	S_1C_1	**S_1C_2**	**S_1C_3**	**S_1C_1**	**S_1C_2**	**S_1C_3**
S_2C_1	0,864	0,659	0,505	0,947	1,404	1,401
S_2C_2	5,051	0,915	0,451	1,097	1,135	1,146
S_2C_3	47,993	1,584	0,706	1,371	1,162	1,036
Mixture of $S_{1\ (IM1\text{-}8C(CN)3}$ and $S_{3\ CBZ\text{-}E}$						
	S_1C_1	**S_1C_2**	**S_1C_3**	**S_1C_1**	**S_1C_2**	**S_1C_3**
S_3C_1	0,731	0,711	0,749	0,969	1,777	2,379
S_3C_2	5,608	1,957	1,129	1,110	2,550	3,967
S_3C_3	51,224	2,563	1,906	1,109	2,393	3,632

4. Discussion

The study revealed several key findings related to the toxicity of ILs and their mixtures with common micropollutants on marine photosynthesizing microorganisms. Exposure to IMI-8C(CN)$_3$, OXTC, CBZ-E, and their mixtures led to significant alterations in pigment composition, growth rate and photosynthetic changes in *M. aeruginosa* and *P. tricornutum*. Both organisms exhibited adaptive responses, such as increased carotenoids and T-SOD upregulation, indicating photoprotection mechanisms.

Numerous studies have previously addressed the toxic activity of Ils towards photosynthesizing microorganisms (Pretti et al., 2009; Latała et al., 2009). The primary focus has been put on acute toxic effects and growth inhibition of freshwater microorganisms (Sanches et al., 2023).

However, recent investigations have provided additional information on the adverse influence of ionic liquids on biochemical responses, such as photosynthetic activity, chlorophyll *a* and *b* content, cell membrane permeability, and cellular ultrastructure (Liu et al., 2018, 2022; Xia et al., 2018; Wang et al., 2022; Deng et al., 2020). The values of the Ils EC_{50} range from 0.01 mg/l for Cl[dmim] for green algae *Scenedesmus obliquus* (Fan et al., 2019a) to 1257.5 mg/l for L-(+)-[emim]L for the freshwater single-cell algae *Euglena gracilis* (Chen et al., 2014), depending on the nature of the cation, the length of the alkyl chain, and the individual sensitivity of the microorganisms. Furthermore, imidazolium heterocyclic rings Ils were found to be more toxic compared to pyridinium and morpholinium ionic liquids (Egorova and Ananikov, 2014; Bubalo et al., 2014).

In our preceding research, we concentrated on analyzing the interactions between the IM1-12Br ionic liquid and OXTC mixture, along with their influence on targeted microorganisms including green algae *Chlorella vulgaris* and bacterium *Aliivibrio fischeri* (Sharma et al., 2023). Substantial impacts were noted on the growth, photosynthetic processes, and pigment content across all the specified microorganisms. Employing the concentration addition and independent action mathematical models, combined with evaluation using the Model Deviation Ratio, enabled the identification of predominantly synergistic interactions within the mixtures studied. The main objective of the previous and current research was to investigate the toxicity of two imidazolium cations with different side chain lengths, namely $[IM18]^+$ and $[IM1–12]^+$. The strong membrane affinity of cations with long alkyl side chains aligns with the "side-chain effect," which describes the decreasing EC_{50} as hydrophobicity increases. This phenomenon has been widely documented for ionic liquids (ILs) across various biological assays (Markiewicz et al., 2011). The selection of the cations was based on the previous studies involving the experimental membrane partitioning of IL cations and estimating their bioconcentration potential (Dołżonek et al., 2017; Maculewicz et al., 2023a). Despite initial indications of a low affinity for biological interphases, the experimental data contradicts this expectation by revealing a considerably higher level of interaction with lipid bilayers. This finding suggests a stronger potential for bioaccumulation of ILs than what could be anticipated based solely on the logarithmic partition coefficient (log K_{ow}) (Dołżonek et al., 2017). The $[IM1-12]^+$ cation exhibits an affinity for membranes based on membrane-water partitioning (log K_{MW}) equal to 3.76 ± 0.04, which can result in rapid sorption to the membrane surface and the insertion of its side chain into the inner region of the membrane. The reported values were higher when compared to log K_{MW} of 2.06 ± 0.15 in case of $[IM1-8]^+$. An even lower log K_{MW} of <1.5 was determined for the $[C(CN)_3]$ anion, showing lower membrane affinity (Dołżonek et al., 2017). Kowalska et al. (2023) aimed to provide an initial understanding of the involvement of the representative blood protein, human serum albumin (HSA), in the potential bioconcentration of ionic liquids. The affinity of $[IM1-8]^+$ to the model protein was confirmed, but it was found to be lower compared to the $[IM1-12]^+$ cation. Further reinforcing these findings, in an in vivo study, it has been established for the first time that long-chain imidazolium ionic liquids are capable of undergoing bioconcentration. The calculated bioconcentration factor (BCF) value for $[IM1-12]^+$, amounting to 21,901 ± 3400 l/kg, categorizes this compound as highly bioaccumulative according to widely accepted criteria. However, the obtained BCF for $[IM1-8]^+$, which falls below 100, indicates a minimal potential for bioconcentration associated with this particular cation (Maculewicz et al., 2023a, 2023b).

In the current study, the effects of binary mixtures of $[IM1-8]^+$ cation paired with a tricyanomethide anion $[C(CN)3]^-$ and two representatives of different classes of commonly detected micropollutants, including a transformation product carbamazepine-10,11-epoxide and antibiotic oxytetracycline, were investigated. Previous evaluation of the biotoxicity of the target cation 1-octyl-3-methylimidazolium $[IM1-8]^+$ and three different anions $[NO3]^{-1}$, $[Cl]^{-1}$, and $[BF4]^{-1}$ against freshwater green algae *Chlorella pyrenoidosa* by Chen et al. (2020) indicated an increase in protein and antioxidant activity along with changes in chlorophyll *a* fluorescence parameters (F_v/F_m), chlorophyll *a* content that resulted in a decrease in photosynthetic efficiency. The results suggested little influence of the anions on the overall toxicity of the cation based on the EC_{50} values of 3.80, 4.72, 4.44 mg/l at 72 h of exposure, respectively. Furthermore, an investigation of the effects of the [IM1-8] + cation in zebrafish embryos (*Danio rerio*) suggested greater bioavailability and accumulation, resulting in oxidative stress and developmental toxicity compared to ionic liquid with a pyridium core (Wang et al., 2022). In the present study, the EC_{50} for $IM1-8C(CN)_3$ was determined to be 0.1 mg/l for *M. aeruginosa* and 8.0 mg/l for *P. tricornutum*. Similarly, IM1-12Br exhibited comparable values of 0.03 mg/l for *M. aeruginosa* and 0.76 mg/l for *P. tricornutum*, as reported by Sharma et al. (2023). Chen et al. (2019) reported 96-h EC_{50} values of 24.0 and 33.6 for 1-octyl-3-methylimidazolium nitrate ($IM1-8NO_3$) and 1-octyl-3-methylimidazolium chloride (IM1-8Cl), respectively, in case of *P. tricornutum*. These values, higher than those found in the present study, suggest the significance of the anion in the overall toxicity.

The available literature concerning mixtures of ILs and other xenobiotics is limited. In a study by Chu et al. (2022), the combination of 1-octyl-3-methylimidazolium chloride (IM1-8Cl) and 1-octyl-3-methylimidazolium bromide with heavy metals resulted in an increased toxicity of ionic liquids (ILs) to the algae *Nostoc punctiforme*. The results indicated that both photosynthesis and growth were significantly affected. In the present investigation, one of the micropollutants selected for mixture toxicity evaluation is a primary metabolite of carbamazepine - a stable anticonvulsant medication that, along with its metabolites, has been widely detected in the aquatic environment, with median concentrations ranging from 2.6 to 22 ng/l in coastal and offshore seawater in the Baltic Sea (Bahlmann et al., 2014; Björlenius et al., 2018; Rajendran and Sen, 2018). Its estimated half-life of 3.5 years in seawater and high persistency make it a valuable indicator of anthropogenic pollution (Brezina et al., 2017). In addition, some of the carbamazepine metabolites have been found to be more toxic than the parent compound (Heye et al., 2016). The human metabolite carbamazepine-10, 11-epoxide has been shown to exhibit slightly weaker toxic effects on the green algae *Raphidocelis subcapitata* as its native form, resulting in 37 % growth inhibition compared to 49 % (Grabarczyk et al., 2020). Its concentration in WWTP effluents ranged from 69 to 2377 ng/l, compared to 4.96 to 175 ng/l of the parent compound (Huerta-Fontela et al., 2010). This situation was also observed in the coastal waters of Norway, where carbamazepine-10, 11-epoxide was found at concentrations of 14 to 77 ng/l, exceeding the levels of the parent compound detected at 20 ng/l (Langford and Thomas, 2011). Its presence was also confirmed in the French coastal waters of the Mediterranean Sea (Martínez Bueno et al., 2016). Carbamazepine-10, 11-epoxide has been found to have a higher potential for bioaccumulation than its native form (Daniele et al., 2017). Recent research indicates that it has an affinity for blood proteins, which may suggest its potential for bioaccumulation based on protein-compound interaction (Kowalska et al., 2021). It has also been found in sediments from which it often can be released back into surface water, indicating high mobility (Li et al., 2015).

The third target compound is oxytetracycline, a ubiquitous antibiotic detected in aquatic environments. Its estimated half-life varies from 151 to 300 days in both upper and deeper marine sediments, as documented by Hektoen et al. (1995). Sediment concentrations of oxytetracycline have been documented as 1.515 μg/g d.w. in the Baltic Sea and 2400 ± 730 μg/kg d.w. in the Mediterranean Sea (Siedlewicz et al., 2018; González-Gaya et al., 2018). Previous studies have reported the value of $EC_{50\ OXTC}$ for the diatom *P. tricornutum* to be 1.73 mg/l, while for *M. aeruginosa*, the values have been observed to be highly dependent on the exposure time, ranging from 0.09 mg/l after 7 days of exposure to 5.4 mg/l after a 24-hour exposure period (Halling-Sørensen, 2000; De Orte et al., 2013; Shang et al., 2015). In this study, the EC_{50} values for *P. tricornutum* and *M. aeruginosa* were found to be 1.5 mg/l and 0.1 mg/l,

respectively, which is consistent with the literature values.

4.1. Chlorophyll a fluorescence

The findings of the study reveal that the applied concentrations of the ionic liquid, in conjunction with the highest level of OXTC, lead to a significant inhibition of the F_v/F_m parameter in both in *M. aeruginosa* and *P. tricornutum*. This outcome suggests an impairment of the photosynthetic activity of cyanobacterial and diatom cells, particularly in relation to the efficiency of photosystem II. The decrease in the F_v/F_m ratio is directly linked to damage to the electron-transfer system and low efficiency of electron transfer between photosystems I and II along with a nonphotochemical quenching increase (Xia et al., 2018). Conversely, lower and medium concentrations of the antibiotic OXTC result in a stimulation of the F_v/F_m parameter in *M. aeruginosa*, indicating a potential adaptive response described in the literature as hormesis effect (Agathokleous et al., 2022). In the case of CBZ-E and both target species, stable F_v/F_m values are observed when exposed to the single compound. However, in most binary mixtures of CBZ-E and IM1-8C$(CN)_3$, a notable decrease in toxicity is observed, as evidenced by F_v/F_m values. This suggests antagonistic interactions between CBZ-E and the ionic liquid, leading to reduced combined effects on the photosynthetic efficiency of microorganism cells, as confirmed by both the CA and IA models. Strong antagonistic interactions are also confirmed by growth changes evaluation in both target microorganisms. The interactions within IM1-8C$(CN)_3$ and OXTC binary mixtures are more complex varying from antagonistic to synergistic depending strongly on the concentration of the compounds. However, antagonistic interactions are more prevalent in all studied OXTC mixtures. Conversely, the increased ET_0/RC, observed under stress conditions, could be attributed to photoprotective mechanisms. These mechanisms might involve adjustments to energy transfer processes as a strategic response to minimize potential damage. Additionally, adaptive strategies could manifest through alterations in pigment composition and antenna size, contributing to a more efficient energy transfer, as evidenced by the increased ET_0/RC ratio. The observed fluctuations in photosynthetic parameters values underscore potentially synergistic or antagonistic interactions within these mixtures, emphasizing the significance of considering the collective impacts of multiple substances on the photosynthetic performance of microorganisms.

4.2. CA and IA models

The differences in the results of the CA and IA models arise primarily from the underlying assumptions of each model and the way they account for interactions between the compounds tested. The CA model – more canonic one - assumes that the pollutants in the mixture act through a similar or related mode of action and can therefore contribute additively to the total toxic effect. In contrast, the IA model assumes that the pollutants act independently of one another, targeting different biological systems or mechanisms (Backhaus et al., 2000). For growth changes in both *M. aeruginosa* and *P. tricornutum*, the CA model indicated strong antagonistic interactions between IMI-8C$(CN)_3$ and OXTC at higher concentrations, with synergistic effects at lower ones; the concentration-dependent variance of MDR in both models appears in all studies especially at NOEC/LOEC levels. This suggest the chemicals share overlapping modes of action and can either mitigate or amplify each other's toxic effects, depending on their relative concentrations. In contrast, the IA model consistently overestimated the toxicity of the mixtures, particularly at higher concentrations of OXTC, but this did not align with the observed antagonistic interactions, especially in CBZ-E mixtures in case of *M. aeruginosa*.

In case of photosynthetic activity, the CA model revealed again a complex interaction pattern; synergistic interactions were observed at the highest concentrations of the ionic liquid, while OXTC exhibited an antagonistic effect at lower concentrations. This indicates that the pollutants interact in a concentration-dependent manner in terms of photosynthetic inhibition. Similar to growth changes, the IA model overestimated toxicity towards photosynthetic activity, particularly where antagonism was present. This is likely due to the IA model's assumption of independent action, which fails to account for interactions that occur between pollutants at different concentrations.

4.3. Pigment composition dynamics and photoprotective mechanisms

Chlorophyll, carotenoids, and phycobilins serve as the primary photosynthetic pigments, facilitating efficient light absorption in algae, and cyanobacteria. These pigments play a crucial role in harvesting light by absorbing it at various wavelengths, enabling photosynthetic organisms to adapt to diverse environments. Chlorophyll pigments, particularly chlorophyll *a*, serve as primary pigments and key indicators of stress responses in ecotoxicological studies (Agathokleous et al., 2020). These pigments are particularly vulnerable to damage due to their central role in the light-harvesting and electron transport processes of photosynthesis. Moreover, oxidative stress can lead to the degradation of chlorophyll *a* into various by-products, such as pheophytin *a* and chlorophyllide *a*, which further impair the photosynthetic efficiency and are often associated with a decrease in the maximum quantum yield of PSII (F_v/F_m) (Agathokleous et al., 2020). Carotenoids contribute to various aspects of photosynthesis, serving roles in light capture and acting as essential antioxidants to mitigate photodamage and photoinhibition. The direct involvement of carotenoids in photochemical reactions is integral to the efficient capture and transfer of light energy during photosynthesis (Polívka and Frank, 2010). Furthermore, carotenoids also fulfill a crucial protective function by acting as antioxidants. They are capable of quenching harmful reactive oxygen species (ROS) that may be generated during photosynthesis due to factors such as environmental stressors, including excess light, high temperatures, nutrient deficiencies, and pollutants (Hasanuzzaman et al., 2020). By neutralizing ROS, carotenoids play a pivotal role in preventing oxidative damage to the photosynthetic apparatus and safeguarding cellular structures from potential photooxidative stress (Hashimoto et al., 2016). Additionally, in response to oxidative stress, organisms may upregulate antioxidant enzymes such as superoxide dismutase (SOD) to mitigate ROS damage. The photoprotective and antioxidant mechanisms of carotenoids can be categorized into four distinct functions: acting as sunscreens, quenching singlet oxygen, dissipating excessive light energy through the xanthophyll cycle, and scavenging radicals. In cyanobacteria, the prominent carotenoids comprise β-carotene, zeaxanthin in hydroxy-derivatives, and echinenone in keto-derivatives (Wada et al., 2013). The observed alterations in pigment production in *M. aeruginosa*, particularly the significant inhibition in the presence of medium (C_2) and highest (C_3) levels of IM1-8C$(CN)_3$, and the substantial increase in pigment content upon exposure to OXTC at all three concentration levels, may be attributed to the differential impacts of these substances on the photosynthetic pathways and metabolic processes of the cyanobacterial cells. In the case of IM1-8C$(CN)_3$, the inhibitory effect on pigment production could be indicative of a disruption in the biosynthetic pathways or a downregulation of enzymes involved in pigment synthesis. Conversely, the considerable increase in pigment content in the presence of OXTC may suggest a stimulatory effect as a response to cellular stress. Oxytetracycline, being an antibiotic, may trigger various cellular responses, including an upregulation of pigment synthesis as a part of the cellular defense mechanism or as a response to oxidative stress. The analysis of binary mixtures of both compounds revealed noteworthy trends in pigment production. The mixtures of C_3 and C_2 showed the decrease of chlorophyll *a* and simultaneous increase in concentrations mainly echinenone and aphanizophyll. This could be attributed to the specific interactions between OXTC and the photosynthetic apparatus, leading to disruptions in chlorophyll *a* synthesis or stability. The significant surge in chlorophyll derivatives production observed in response to mixture treatments with the highest OXTC

concentration may indicate presence of adaptive responses or compensatory mechanisms. The exposure of *M. aeruginosa* to CBZ-E did not yield statistically significant changes in pigment ratios. Interestingly, the combination of $C_{1\ CBZ\text{-}E}$ and $C_{1\ IM1\text{-}8C(CN)3}$ stimulated chlorophyll *a* production. The mixture treatments, especially those with the highest IL concentration, induced significant alterations in pigment ratios and chlorophyll *a* content in cyanobacterium. The observed elevation in chlorophyllide *a* pigment content in cyanobacterium in the presence of ionic liquid, antibiotic, and their binary mixtures, as well as IL and CBZ-E mixtures, may be indicative of a disturbance in the chlorophyll biosynthesis process. Chlorophyllide *a* serves as a precursor to chlorophyll, and its accumulation suggests a potential disruption in the conversion of chlorophyllide *a* to mature chlorophyll *a* molecules (Sobotka, 2014; Kopečná et al., 2013). This phenomenon could be a response to stress, wherein the normal chlorophyll *a* biosynthesis pathway is altered, leading to the accumulation of intermediate products such as chlorophyllide *a*. Overall, the specific interactions between CBZ-E, OXTC, and IM1-8C$(CN)_3$ played a crucial role in modulating the photosynthetic pigment composition.

Under varied environmental conditions with fluctuating light quantities, phycobilins capture a broad spectrum of light, allowing cyanobacteria to thrive in deep waters. Cyanobacteria construct a distinctive light-harvesting structure known as the phycobilisome, associated with photosystem II to facilitate the transfer of light energy (Adir et al., 2020). The size and protein composition of the phycobilisome undergo alterations in response to variations in environmental conditions. Phycoerythrin (PE) is the predominant phycobiliprotein found in numerous red algae and certain cyanobacteria. It is distinguished by its robust light absorption in the green spectrum (480–570 nm) and emits intense fluorescence around 575–580 nm. Phycocyanin exhibits a high capacity for absorbing light, particularly within the range of 580 to 630 nm, and releases vivid red fluorescence in the wavelength range of 635–645 nm (Stadnichuk et al., 2015). The sharp increase in phycobiliproteins content in response to the presence of xenobiotics can be explained through adaptive strategies of cyanobacterium, including the cellular stress response involving the upregulation of proteins. Phycobilins, particularly phycocyanin, have been identified as antioxidants capable of scavenging reactive oxygen species (ROS) generated during oxidative stress (Wada et al., 2013). In the presence of IM1-8C$(CN)_3$, OXTC, and their binary mixtures, there was an observed increase in the production of phycobiliproteins. This upregulation is likely a defense mechanism against oxidative stress, as further corroborated by the Total Superoxide Dismutase (T-SOD) values. A rapid increase in their production may be an adaptive response to optimize light absorption and energy transfer, potentially compensating for any disruptions caused by the presence of micropollutants. In the case of mixture of the highest concentration of ionic liquid with $C_{3\ OXTC}$, a decrease in phycoerythrin can be observed. Cellular stress and the disruption of chlorophyll *a* could consequently affect the stability and functionality of phycobiliproteins, leading to their overall decrease. Similar observations were reported by Chang et al. (2023) in marine red algae *Sarcodia suiae* exposed to heavy metals. The exposure of *M. aeruginosa* to medium and highest concentrations of CBZ-E led to distinct changes in phycobilins ratios, specifically an increase in phycoerythrin relative levels and a decrease in phycocyanin relative concentration. Conversely, the exposure to CBZ-E alone did not result in statistically significant alterations in other pigment ratios, including chlorophyll *a*. These alterations are indicative of the sensitivity of phycobiliproteins as responsive markers to stress conditions induced by CBZ-E. Interestingly, in the binary mixtures featuring the highest concentrations of both analytes, phycocyanin was entirely absent, emphasizing a specific and complex response to this particular combination of micropollutants. Due to its specific sensitivity and fluorescence quenching ability, phycocyanin has been considered an effective alternative method for detecting trace levels of metals, including Hg^{2+}, in aquatic systems (Bhayani et al., 2016). The finding of the current study further confirm its utility as a responsive biomarker for environmental monitoring.

To prevent photoinhibition, *P. tricornutum* cells engage in the synthesis of carotenoids, including β,β-carotene, diadinoxanthin, diatoxanthin, as well as violaxanthin, and zeaxanthin as documented by Kuczyńska et al. (2015, 2020). These carotenoids play a dual role, serving as accessory light-harvesting pigments. In case of *P. tricornutum*, the exposure to CBZ-E elicited significant rises in diadinoxanthin levels, indicating the initiation of a Non-Photochemical Quenching (NPQ) energy dissipation pathway governed by diadinoxanthin. Non-Photochemical Quenching (NPQ) is a vital photoprotective mechanism employed by photosynthetic organisms, including plants and algae, to dissipate excess absorbed light energy as heat. In response to environmental stressors, diadinoxanthin undergoes structural changes that allow it to safely dissipate the excess energy as heat, thereby preventing the formation of potentially harmful reactive oxygen species and protecting the photosynthetic machinery from damage. The diadinoxanthin cycle, recognized as the principal short-term photoprotective mechanism in diatoms, plays a pivotal role in safeguarding the photosynthetic apparatus (Bertrand, 2010; Lacour et al., 2020). Collectively, these findings suggest that *P. tricornutum* safeguards the photosynthetic processes from the impacts of micropollutants by employing short-term photoacclimation strategies, including an increase in the concentration of pigments associated with NPQ along with the upregulation of T-SOD. Similar observations were noted in the freshwater diatom *Fragilaria crotonensis* during pH-induced photostress (Zepernick et al., 2022). The diatom *P. tricornutum* exhibits significant responses to the presence of CBZ-E and the ionic liquid binary mixtures, especially at higher concentrations. The demise of diatom cells can be characterized by a cessation of vital cellular processes, leading to a decline in overall cell viability. This can manifest as a lack of pigment production, wherein the usual synthesis of pigments crucial for photosynthetic activities is disrupted. The observed growth inhibition further indicates a compromised ability of diatom cells to proliferate and thrive. In the context of OXTC and its binary mixtures, the observed increase in pigment relative levels suggests the activation of adaptive responses and stress-induced mechanisms. These changes in pigment composition are likely strategic measures serving in photoprotection and energy dissipation, aimed at mitigating the impact of stress on the photosynthetic apparatus. The documented increases in β-carotene, diatoxanthin, and violaxanthin relative levels signify the diatom's endeavor to acclimate and uphold cellular homeostasis under the influence of target micropollutants. Overall, alongside pigment upregulation and changing dynamics, the overproduction of superoxide dismutase (SOD) was observed as a primary mechanism for protection against oxidative stress. The substantial decrease in T-SOD activity at higher concentrations of ionic liquid and mixture treatments in both *M. aeruginosa* and *P. tricornutum* can be attributed to the high accumulation of the superoxide radical, derived from an imbalance between detoxification and production of the ability of SOD to respond to radical levels.

5. Conclusions

The study employed a comprehensive approach, analyzing chlorophyll *a* fluorescence parameters as indicators of photosynthetic activity in selected microorganisms, alongside their pigment profiles, including chlorophylls, xanthophylls, carotenes, and phycobilins, as well as oxidative stress responses to binary mixtures of target micropollutants including the antibiotic oxytetracycline, the metabolite carbamazepine 10,11-epoxide, and the imidazolium ionic liquid IM1-8C$(CN)_3$.

The results revealed alterations in pigment production, indicating the impact of these substances on photosynthetic pathways and metabolic processes in the microorganisms. These findings are supported by changes in chlorophyll *a* fluorescence-specific parameters, which suggest an impairment of photosynthetic activity, particularly influencing the functionality of photosystem II. The observed changes in pigment levels suggest that *P. tricornutum* safeguards its photosynthetic processes

from micropollutant impacts through short-term photoacclimation strategies, including the upregulation of pigments associated with non-photochemical quenching (NPQ). The increase in chlorophyllide *a* relative pigment content in response to binary mixtures of all target compounds could suggest a disruption in the chlorophyll *a* biosynthesis process. Exposure of *M. aeruginosa* to low concentrations of CBZ-E led to significant changes in phycobilin ratios, specifically increasing phycoerythrin and decreasing phycocyanin, indicating the sensitivity of phycobiliproteins as stress markers, while other pigment ratios, including chlorophyll *a*, remained unaffected. The investigation identified predominantly antagonistic interactions within the studied mixtures, based on observations of photosynthetic activity and growth inhibition.

Aquatic ecosystems are continuously exposed to complex mixtures of micropollutants, which can lead to unpredictable effects, particularly in sensitive and fragile closed or semi-closed environments such as the brackish Baltic Sea, which experiences significant anthropogenic pressure. The results of the present study underscore the necessity of evaluating the combined effects of multiple pollutants, as interactions between different compounds can significantly influence their toxicity towards nontarget organisms and, consequently, their overall environmental impact. Moreover, most current research tends to focus on short-term effects. Therefore, long-term and chronic exposure studies are crucial for understanding the cumulative impacts of micropollutants on ecosystems. The scientific focus should involve the study of more complex mixtures of micropollutants present at low concentrations, reflecting real-world scenarios, and evaluating their impact on a broader range of organisms. This approach should be complemented by the development and application of advanced modeling tools that can simulate the interactions and cumulative effects.

CRediT authorship contribution statement

Lilianna Sharma: Writing – original draft, Investigation, Conceptualization. **Błażej Kudłak:** Writing – review & editing, Investigation, Conceptualization. **Joanna Stoń-Egiert:** Writing – review & editing, Investigation. **Grzegorz Siedlewicz:** Writing – review & editing, Conceptualization. **Ksenia Pazdro:** Writing – review & editing, Supervision, Conceptualization.

Declaration of competing interest

The authors declare the following financial interests/personal relationships which may be considered as potential competing interests: Lilianna Sharma reports financial support was provided by Institute of Oceanology Polish Academy of Sciences. Lilianna Sharma reports a relationship with National Science Centre Poland that includes: funding grants. If there are other authors, they declare that they have no known competing financial interests or personal relationships that could have appeared to influence the work reported in this paper.

Acknowledgments

The authors acknowledge the financial support of the National Science Centre (Poland) under the decision NCN 2021/41/N/NZ9/00315 and statutory funds from the Institute of Oceanology (task II.2 and II.3).

We thank Patrycja Kwiecień and Anna Malenga for their assistance in laboratory work.

Appendix A. Supplementary data

Supplementary data to this article can be found online at https://doi.org/10.1016/j.scitotenv.2024.177080.

Data availability

Data will be made available on request.

References

Adir, N., Bar-Zvi, S., Harris, D., 2020. The amazing phycobilisome. Biochim. Biophys. Acta Bioenerg. 1861 (4), 148047. https://doi.org/10.1016/j.bbabio.2019.07.002, 1.

Agathokleous, E., Feng, Z., Peñuelas, J., 2020. Chlorophyll hormesis: are chlorophylls major components of stress biology in higher plants? Sci. Total Environ. 726, 138637. https://doi.org/10.1016/j.scitotenv.2020.138637.

Agathokleous, E., Wang, Q., Iavicoli, I., Calabrese, E.J., 2022. The relevance of hormesis at higher levels of biological organization: hormesis in microorganisms. Current Opinion in Toxicology. 29, 1–9. https://doi.org/10.1016/j.cotox.2021.11.001.

Backhaus, T., 2014. Medicines, shaken and stirred: a critical review on the ecotoxicology of pharmaceutical mixtures. Philos. Trans. R Soc. Lond. B Biol. Sci. 369 (1656), 20130585. https://doi.org/10.1098/rstb.2013.0585, 19.

Backhaus, T., Altenburger, R., Boedeker, W., Faust, M., Scholze, M., Grimme, L.H., 2000. Predictability of the toxicity of a multiple mixture of dissimilarly acting chemicals to *Vibrio fischeri*. Environ.Toxicol. Chem. 19, 2348–2356. https://doi.org/10.1002/etc.5620190927.

Bahlmann, A., Brack, W., Schneider, R.J., Krauss, M., 2014. Carbamazepine and its metabolites in wastewater: analytical pitfalls and occurrence in Germany and Portugal. Water Res. 15 (57), 104–114. https://doi.org/10.1016/j.watres.2014.03.022.

Barbosa, M.O., Moreira, N.F.F., Ribeiro, A.R., Pereira, M.F.R., Silva, A.M.T., 2016. Occurrence and removal of organic micropollutants: an overview of the watch list of EU Decision 2015/495. Water Res. 1 (94), 257–279. https://doi.org/10.1016/j.watres.2016.02.047.

Bertrand, M., 2010. Carotenoid biosynthesis in diatoms. Photosynth. Res. 106, 89–102. https://doi.org/10.1007/s11120-010-9589-x.

Bhayani, K., Mitra, M., Ghosh, T., Mishra, S., 2016. C-Phycocyanin as a potential biosensor for heavy metals like Hg 2+ in aquatic systems. RSC Adv. 6 (112), 111599–111605. https://doi.org/10.1039/C6RA22753H.

Björlenius, B., Ripszám, M., Haglund, P., Lindberg, R.H., Tysklind, M., Fick, J., 2018. Pharmaceutical residues are widespread in Baltic Sea coastal and offshore waters – screening for pharmaceuticals and modeling of environmental concentrations of carbamazepine. Sci. Total Environ. 633, 1496–1509. https://doi.org/10.1016/j.scitotenv.2018.03.276.

Bliss, C., 1939. The toxicity of poisons applied jointly. Ann. Appl. Biol. 26, 585–615. https://doi.org/10.1111/j.1744-7348.1939.tb06990.x.

Bradford, M.M., 1976. A rapid and sensitive method for the quantitation of microgram quantities of protein utilizing the principle of protein-dye binding. Anal. Biochem. 7 (72), 248–254. https://doi.org/10.1006/abio.1976.9999.

Brezina, E., Prasse, C., Meyer, J., Mückter, H., Ternes, T.A., 2017. Investigation and risk evaluation of the occurrence of carbamazepine, oxcarbazepine, their human metabolites and transformation products in the urban water cycle. Environ. Pollut. 225, 261–269. https://doi.org/10.1016/j.envpol.2016.10.106.

Bubalo, M.C., Radošević, K., Redovniković, I.R., Halambek, J., Srček, V.G., 2014. A brief overview of the potential environmental hazards of ionic liquids. Ecotoxicol. Environ. Saf. 99, 1–12. https://doi.org/10.1016/j.ecoenv.2013.10.019.

Chang, C.C., Tseng, C.C., Han, T.W., Barus, B.S., Chuech, J.Y., Cheng, S.Y., 2023. Effects of lead and zinc exposure on uptake and exudation levels, chlorophyll-a, and phycobiliproteins in *Sarcodia suiae*. Int. J. Environ. Res. Public Health 20 (4), 2821. https://doi.org/10.3390/ijerph20042821.

Chen, H., Zou, Y., Zhang, L., Wen, Y., Liu, W., 2014. Enantioselective toxicities of chiral ionic liquids 1-alkyl-3-methylimidazolium lactate to aquatic algae. Aquat. Toxicol. 154, 114–120. https://doi.org/10.1016/j.aquatox.2014.05.010.

Chen, B., Xue, C., Amoah, P.K., Li, D., Gao, K., Deng, X., 2019. Impacts of four ionic liquids exposure on a marine diatom *Phaeodactylum tricornutum* at physiological and biochemical levels. Sci. Total Environ. 665, 492–501. https://doi.org/10.1016/j.scitotenv.2019.02.020.

Chen, B., Dong, J., Li, B., Xue, C., Tetteh, P.A., Li, D., Gao, K., Deng, X., 2020. Using a freshwater green alga *Chlorella pyrenoidosa* to evaluate the biotoxicity of ionic liquids with different cations and anions. Ecotoxicol. Environ. Saf. 198, 110604. https://doi.org/10.1016/j.ecoenv.2020.110604.

Cho, C.W., Pham, T.P.T., Zhao, Y., Stolte, S., Yun, Y.S., 2021. Review of the toxic effects of ionic liquids. Sci. Total Environ. 10 (786), 147309. https://doi.org/10.1016/j.scitotenv.2021.147309.

Chu, L., Hou, X., Song, X., Zhao, X., 2022. Toxicological effects of different ionic liquids on growth, photosynthetic pigments, oxidative stress, and ultrastructure of *Nostoc punctiforme* and the combined toxicity with heavy metals. Chemosphere 298, 134273. https://doi.org/10.1016/j.chemosphere.2022.134273.

Clayton, J.J.R., Dortch, Q., Thoresen, S.S., Ahmed, S.I., 1988. Evaluation of methods for the separation and analysis of proteins and free amino acids in phytoplankton samples. J. Plankton Res. 10 (3), 341–358. https://doi.org/10.1093/plankt/10.3.341.

Daniele, G., Fieu, M., Joachim, S., Bado-Nilles, A., Beaudouin, R., Baudoin, P., James-Casas, A., Andres, S., Bonnard, M., Bonnard, I., Geffard, A., Vulliet, E., 2017. Determination of carbamazepine and 12 degradation products in various compartments of an outdoor aquatic mesocosm by reliable analytical methods based on liquid chromatography-tandem mass spectrometry. Environ. Sci. Pollut. Res. Int. 24 (20), 16893–16904. https://doi.org/10.1007/s11356-017-9297-6.

De Orte, M.R., Carballeira, C., Viana, I.G., Carballeira, A., 2013. Assessing the toxicity of chemical compounds associated with marine land-based fish farms: the use of mini-scale microalgal toxicity tests. Chem. Ecol. 29 (6), 554–563. https://doi.org/10.1080/02757540.2013.790381.

Deng, Y., Beadham, I., Ren, H.Y., Ji, M.M., Ruan, W.Q., 2020. A study into the species sensitivity of green algae towards imidazolium-based ionic liquids using flow

cytometry. Ecotoxicol. Environ. Saf. 194, 110392. https://doi.org/10.1016/j.ecoenv.2020.110392.
Dołżonek, J., Cho, C.W., Stepnowski, P., Markiewicz, M., Thöming, J., Stolte, S., 2017. Membrane partitioning of ionic liquid cations, anions and ion pairs - estimating the bioconcentration potential of organic ions. Environ. Pollut. 228, 378–389. https://doi.org/10.1016/j.envpol.2017.04.079.
Drakvik, E., Altenburger, R., Aoki, Y., Backhaus, T., Bahadori, T., Barouki, R., Brack, W., Cronin, M.T.D., Demeneix, B., Hougaard, Bennekou, S., van Klaveren, J., Kneuer, C., Kolossa-Gehring, M., Lebret, E., Posthuma, L., Reiber, L., Rider, C., Rüegg, J., Testa, G., van der Burg, B., van der Voet, H., Warhurst, A.M., van de Water, B., Yamazaki, K., Öberg, M., Bergman, Å., 2020. Statement on advancing the assessment of chemical mixtures and their risks for human health and the environment. Environ. Int. 134, 105267. https://doi.org/10.1016/j.envint.2019.105267.
ECHA, 2008. Guidance on Information Requirements and Chemical Safety Assessment Chapter R.10: Characterisation of Dose [Concentration]-response for Environment. European Chemicals Agency (ECHA), Helsinki, Finland. https://echa.europa.eu/guidance-documents/guidance-on-information-requirements-and-chemical-safety-assessment (Accessed on 15 October 2024).
Egorova, K.S., Ananikov, V.P., 2014. Toxicity of ionic liquids: eco(cyto)activity as complicated, but unavoidable parameter for task-specific optimization. ChemSusChem 7 (2), 336–360. https://doi.org/10.1002/cssc.201300459.
Fan, H., Jin, M., Wang, H., Xu, Q., Xu, L., Wang, C., Du, S., Liu, H., 2019a. Effect of differently methyl-substituted ionic liquids on *Scenedesmus obliquus* growth, photosynthesis, respiration, and ultrastructure. Environ. Pollut. 250, 155–165. https://doi.org/10.1016/j.envpol.2019.04.021.
Fan, H., Liu, H., Dong, Y., Chen, C., Wang, Z., Guo, J., Du, S., 2019b. Growth inhibition and oxidative stress caused by four ionic liquids in *Scenedesmus obliquus*: role of cations and anions. Sci. Total Environ. 15, 570–579. https://doi.org/10.1016/j.scitotenv.2018.09.106.
Ghanem, O.B., Papaiconomou, N., Mutalib, A., Viboud, S., El-Harbawi, M., Uemura, Y., Gonfa, G., Bustam, M.A., Lévêque, J.M., 2015. Thermophysical properties and acute toxicity towards green algae and *Vibrio fischeri* of amino acid-based ionic liquids. J Mol Liquids. 212, 352–359. https://doi.org/10.1016/j.molliq.2015.09.017.
González-Gaya, B., Cherta, L., Nozal, L., Rico, A., 2018. An optimized sample treatment method for the determination of antibiotics in seawater, marine sediments and biological samples using LC-TOF/MS. Sci. Total Environ. 1 (643), 994–1004. https://doi.org/10.1016/j.scitotenv.2018.06.079.
Grabarczyk, Ł., Mulkiewicz, E., Stolte, S., Puckowski, A., Pazda, M., Stepnowski, P., Białk-Bielińska, A., 2020. Ecotoxicity screening evaluation of selected pharmaceuticals and their transformation products towards various organisms. Environ. Sci. Pollut. Res. 27, 26103–26114. https://doi.org/10.1007/s11356-020-08881-3.
Guillard, R.R.L., 1975. Culture of phytoplankton for feeding marine invertebrates. In: Smith, W.L., Chanley, M.H. (Eds.), Culture of Marine Invertebrate Animals. Plenum Press, New York, pp. 26–60. https://doi.org/10.1007/978-1-4615-8714-9_3.
Hajji, A.L., Lucas, K.N., 2024. Anthropogenic stressors and the marine environment: from sources and impacts to solutions and mitigation. Mar. Pollut. Bull. 205, 116557. https://doi.org/10.1016/j.marpolbul.2024.116557.
Halling-Sørensen, B., 2000. Algal toxicity of antibacterial agents used in intensive farming. Chemosphere 40 (7), 731–739. https://doi.org/10.1016/s0045-6535(99)00445-2.
Hasanuzzaman, M., Bhuyan, M.H.M.B., Zulfiqar, F., Raza, A., Mohsin, S.M., Mahmud, J. A., Fujita, M., Fotopoulos, V., 2020. Reactive oxygen species and antioxidant defense in plants under abiotic stress: revisiting the crucial role of a universal defense regulator. Antioxidants (Basel). 9 (8), 681. https://doi.org/10.3390/antiox9080681, 29.
Hashimoto, H., Uragami, C., Cogdell, R.J., 2016. Carotenoids and photosynthesis. Subcell. Biochem. 79, 111–139. https://doi.org/10.1007/978-3-319-39126-7_4.
Hayes, A.W., Li, R., Hoeng, J., Iskandar, A., Peistch, M.C., Dourson, M.L., 2019. New approaches to risk assessment of chemical mixtures. Toxicology Research and Application. https://doi.org/10.1177/2397847318820768.
Hektoen, H., Berge, J.A., Hormazabal, V., Yndestad, M., 1995. Persistence of antibacterial agents in marine sediments. Aquaculture 133, 175–184. https://doi.org/10.1016/0044-8486(94)00310-K.
Heye, K., Becker, D., Lütke Eversloh, C., Durmaz, V., Ternes, T.A., Oetken, M., Oehlmann, J., 2016. Effects of carbamazepine and two of its metabolites on the non-biting midge *Chironomus riparius* in a sediment full life cycle toxicity test. Water Res. 98, 19–27. https://doi.org/10.1016/j.watres.2016.03.071.
Huerta-Fontela, M., Galceran, M.T., Ventura, F., 2010. Fast liquid chromatography–quadrupole-linear ion trap mass spectrometry for the analysis of pharmaceuticals and hormones in water resources. J. Chromatogr. A 1217 (25), 4212–4222. https://doi.org/10.1016/j.chroma.2009.11.007.
Jin, M., Wang, H., Li, Z., Fu, L., Chu, L., Wu, J., Du, S., Liu, H., 2019. Physiological responses of *Chlorella pyrenoidosa* to 1-hexyl-3-methyl chloride ionic liquids with different cations. Sci. Total Environ. 685, 315–323. https://doi.org/10.1016/j.scitotenv.2019.05.303.
Kaur, G., Kumar, H., Singla, M., 2022. Diverse applications of ionic liquids: a comprehensive review. J. Mol. Liq. 351, 118556. https://doi.org/10.1016/j.molliq.2022.118556.
Kopečná, J., Sobotka, R., Komenda, J., 2013. Inhibition of chlorophyll biosynthesis at the protochlorophyllide reduction step results in the parallel depletion of photosystem I and photosystem II in the cyanobacterium *Synechocystis* PCC 6803. Planta 237 (2), 497–508. https://doi.org/10.1007/s00425-012-1761-4.
Kowalska, D., Maculewicz, J., Stepnowski, P., Dołżonek, J., 2021. Interaction of pharmaceutical metabolites with blood proteins and membrane lipids in the view of bioconcentration: a preliminary study based on in vitro assessment. Sci. Total Environ. 20 (783), 146987. https://doi.org/10.1016/j.scitotenv.2021.146987.
Kowalska, D., Dołżonek, J., Żamojć, K., Samsonov, S.A., Maszota-Zieleniak, M., Makowska, J., Stepnowski, P., Białk-Bielińska, A., Wyrzykowski, D., 2023. Insights into the interaction of human serum albumin with ionic liquids - thermodynamic, spectroscopic and molecular modelling studies. Int. J. Biol. Macromol. 25 (249), 125883. https://doi.org/10.1016/j.ijbiomac.2023.125883.
Kuczyńska, P., Jemioła-Rzemińska, M., Strzałka, K., 2015. Photosynthetic pigments in diatoms. Mar. Drugs 13, 5847–5881. https://doi.org/10.3390/md13095847.
Kuczyńska, P., Jemioła-Rzemińska, M., Nowicka, B., Jakubowska, A., Strzałka, W., Burda, K., Strzałka, K., 2020. The xanthophyll cycle in diatom *Phaeodactylum tricornutum* in response to light stress. Plant Physiol. Biochem. 7 (152), 125–137. https://doi.org/10.1016/j.plaphy.2020.04.043.
Lacour, T., Babin, M., Lavaud, J., 2020. Diversity in xanthophyll cycle pigments content and related nonphotochemical quenching (NPQ) among microalgae: implications for growth strategy and ecology. J. Phycol. 56 (2), 245–263. https://doi.org/10.1111/jpy.12944.
Langford, K., Thomas, K.V., 2011. Input of selected human pharmaceutical metabolites into the Norwegian aquatic environment. J. Environ. Monit. 13 (2), 416–421. https://doi.org/10.1039/c0em00342e.
Latała, A., Nędzi, M., Stepnowski, P., 2009. Toxicity of imidazolium and pyridinium based ionic liquids towards algae. *Bacillaria paxillifer* (a microphytobenthic diatom) and *Geitlerinema amphibium* (a microphytobenthic blue green alga). Green Chem. 11 (9), 1371–1376. https://doi.org/10.1039/b901887e.
Leitch, A.C., Abdelghany, T.M., Probert, P.M., Dunn, M.P., Meyer, S.K., Palmer, J.M., Cooke, M.P., Blake, L.I., Morse, K., Rosenmai, A.K., Oskarsson, A., Bates, L., Figueiredo, R.S., Ibrahim, I., Wilson, C., Abdelkader, N.F., Jones, D.E., Blain, P.G., Wright, M.C., 2020. The toxicity of the methylimidazolium ionic liquids, with a focus on M8OI and hepatic effects. Food Chem. Toxicol. 136, 111069. https://doi.org/10.1016/j.fct.2019.111069.
Leitch, A.C., Ibrahim, I., Abdelghany, T.M., Charlton, A., Roper, C., Vidler, D., Palmer, J. M., Wilson, C., Jones, D.E., Blain, P.G., Wright, M.C., 2021. The methylimidazolium ionic liquid M8OI is detectable in human sera and is subject to biliary excretion in perfused human liver. Toxicology 459, 152854. https://doi.org/10.1016/j.tox.2021.152854.
Li, Z., Sobek, A., Radke, M., 2015. Flume experiments to investigate the environmental fate of pharmaceuticals and their transformation products in streams. Environ. Sci. Technol. 49 (10), 6009–6017. https://doi.org/10.1021/acs.est.5b00273.
Liu, D., Liu, H., Wang, S., Chen, J., Xia, Y., 2018. The toxicity of ionic liquid 1-decylpyridinium bromide to the algae *Scenedesmus obliquus*: growth inhibition, phototoxicity, and oxidative stress. Sci. Total Environ. 622-623, 1572–1580. https://doi.org/10.1016/j.scitotenv.2017.10.021.
Liu, Y., Zhang, Y., Sultan, Y., Xiao, P., Yang, L., Lu, H., Zhang, B., 2022. Inhibition effect of ionic liquid [Hmim]Cl on *Microcystis* growth and toxin production. Int. J. Environ. Res. Public Health 19 (14), 8719. https://doi.org/10.3390/ijerph19148719, 18.
Lyman, J., Fleming, R.H., 1940. Composition of sea water. J. Mar. Res. 3, 134–146. https://elischolar.library.yale.edu/journal_of_marine_research/566.
Maculewicz, J., Świacka, K., Stepnowski, P., Dołżonek, J., Białk-Bielinska, 2022. Ionic liquids as potentially hazardous pollutants: evidences of their presence in the environment and recent analytical developments. J. Hazard. Mater. 5 (437), 129353. https://doi.org/10.1016/j.jhazmat.2022.129353.
Maculewicz, J., Dołżonek, J., Sharma, L., Białk-Bielinska, A., Stepnowski, P., Pazdro, K., 2023a. Bioconcentration of imidazolium ionic liquids: in vivo evaluation in marine mussels *Mytilus trossulus*. Sci. Total Environ. 858, 159388. https://doi.org/10.1016/j.scitotenv.2022.159388.
Maculewicz, J., Stepnowski, P., Dołżonek, J., Białk-Bielinska, A., 2023b. Analysis of imidazolium ionic liquids in biological matrices: a novel procedure for the determination of trace amounts in marine mussels. Talanta 252, 123790. https://doi.org/10.1016/j.talanta.2022.123790.
Markiewicz, M., Stolte, S., Lustig, Z., Łuczak, J., Skup, M.M., Hupka, J., Jungnickel, C., Luczak, J., 2011. Influence of microbial adaption and supplementation of nutrients on the biodegradation of ionic liquids in sewage sludge treatment processes. J. Hazard. Mater. 195, 378e382. https://doi.org/10.1016/j.jhazmat.2011.08.053.
Martínez Bueno, M.J., Herrera, S., Munaron, D., Boillot, C., Fenet, H., Chiron, S., Gómez, E., 2016. POCIS passive samplers as a monitoring tool for pharmaceutical residues and their transformation products in marine environment. Environ. Sci. Pollut. Res. Int. 23 (6), 5019–5029. https://doi.org/10.1007/s11356-014-3796-5.
Moreno-González, R., Rodríguez-Mozaz, S., Gros, M., Pérez-Cánovas, E., Barceló, D., León, V.M., 2014. Input of pharmaceuticals through coastal surface watercourses into a Mediterranean lagoon (Mar Menor, SE Spain): sources and seasonal variations. Sci. Total Environ. 15 (490), 59–72. https://doi.org/10.1016/j.scitotenv.2014.04.097.
Moreno-González, R., Rodriguez-Mozaz, S., Gros, M., Barceló, D., León, V.M., 2015. Seasonal distribution of pharmaceuticals in marine water and sediment from a Mediterranean coastal lagoon (SE Spain). Environ. Res. 138, 326–344. https://doi.org/10.1016/j.envres.2015.02.016.
Neumann, M., Schliebner, I., 2019. Protecting the Sources of Our Drinking Water: The criteria for Identifying Persistent, Mobile, and Toxic (PMT) Substances and Very Persistent, and Very Mobile (vPvM) Substances Under the EU Chemical Legislation REACH. UBA Texte 127/2019. ISSN: 1862-4804. German Environmental Agency (UBA), Dessau-Rosslau, Germany. https://www.umweltbundesamt.de/sites/default/files/medien/1410/publikationen/2019-11-29_texte_127-2019_protecting-sources-drinking-water-pmt.pdf. Accessed 20 August 2024.
Neuwald, I., Muschket, M., Zahn, D., Berger, U., Seiwert, B., Meier, T., Kuckelkorn, J., Strobel, C., Knepper, T.P., Reemtsma, T., 2021. Filling the knowledge gap: a suspect screening study for 1310 potentially persistent and mobile chemicals with SFC- and

HILIC-HRMS in two German river systems. Water Res. 1 (204), 117645. https://doi.org/10.1016/j.watres.2021.117645.
OECD, 2011. Test No. 201: freshwater alga and cyanobacteria, growth inhibition test. In: OECD Guidelines for the Testing of Chemicals in Section 2: Effects on Biotic Systems. https://doi.org/10.1787/20745761.
Oskarsson, A., Wright, M.C., 2019. Ionic liquids: new emerging pollutants, similarities with perfluorinated alkyl substances (PFASs). Environ. Sci. Technol. 53 (18), 10539–10541. https://doi.org/10.1021/acs.est.9b04778, 17.
Peterson, G.L., 1977. A simplification of the protein assay method of Lowry et al. which is more generally applicable. Anal. Biochem. 83 (2), 346–356. https://doi.org/10.1016/S0076-6879(83)91014-5.
Peterson, G.L., 1983. Determination of total protein. Methods Enzymol. 91, 95–119. https://doi.org/10.1016/s0076-6879(83)91014-5.
Pinto, I., Simões, M., Gomes, I.B., 2022. An overview of the impact of pharmaceuticals on aquatic microbial communities. Antibiotics (Basel). 11 (12), 1700. https://doi.org/10.3390/antibiotics11121700, 25.
Plackett, R., Hewlett, P., 1952. Quantal responses to mixtures of poisons. J. R. Stat. Soc. Ser. B (Methodological). 14, 141–163. https://doi.org/10.1111/j.2517-6161.1952.tb00108.x.
Polívka, T., Frank, H.A., 2010. Molecular factors controlling photosynthetic light harvesting by carotenoids. Acc. Chem. Res. 43 (8), 1125–1134. https://doi.org/10.1021/ar100030m, 17.
Pretti, C., Chiappe, C., Baldetti, I., Brunini, S., Monni, G., Intorre, L., 2009. Acute toxicity of ionic liquids for three freshwater organisms: *Pseudokirchneriella subcapitata*, *Daphnia magna* and *Danio rerio*. Ecotoxicol. Environ. Saf. 72 (4), 1170–1176. https://doi.org/10.1016/j.ecoenv.2008.09.01.
Probert, P.M., Leitch, A.C., Dunn, M.P., Meyer, S.K., Palmer, J.M., Abdelghany, T.M., Lakey, A.F., Cooke, M.P., Talbot, H., Wills, C., McFarlane, W., Blake, L.I., Rosenmai, A.K., Oskarsson, A., Figueiredo, R., Wilson, C., Kass, G.E., Jones, D.E., Blain, P.G., Wright, M.C., 2018. Identification of a xenobiotic as a potential environmental trigger in primary biliary cholangitis. J. Hepatol. 69 (5), 1123–1135. https://doi.org/10.1016/j.jhep.2018.06.027.
Qureshi, Z.S., Deshmukh, K.M., Bhanage, B.M., 2014. Applications of ionic liquids in organic synthesis and catalysis. Clean Techn. Environ. Policy 16, 1487–1513. https://doi.org/10.1007/s10098-013-0660-0.
Rajendran, K., Sen, S., 2018. Adsorptive removal of carbamazepine using biosynthesized hematite nanoparticles. Environmental Nanotechnology, Monitoring & Management 9, 122–127. https://doi.org/10.1016/j.enmm.2018.01.001brez.
Roháček, K., Soukupová, J., Barták, M., 2008. Chlorophyll fluorescence: a wonderful tool to study plant physiology and plant stress. In: Schoefs, B. (Ed.), Plant Cell Compartments. Research Signpost, Kerala, pp. 41–104.
Russo, M.T., Rogato, A., Jaubert, M., Karas, B.J., Falciatore, A., 2023. *Phaeodactylum tricornutum*: an established model species for diatom molecular research and an emerging chassis for algal synthetic biology. J. Phycol. 59 (6), 1114–1122. https://doi.org/10.1111/jpy.13400.
Sanches, M.V., Freitas, R., Oliva, M., Cuccaro, A., Monni, G., Mezzetta, A., Guazzelli, L., Pretti, C., 2023. Toxicity of ionic liquids in marine and freshwater microorganisms and invertebrates: state of the art. Environ. Sci. Pollut. Res. Int. 30 (14), 39288–39318. https://doi.org/10.1007/s11356-023-25562-z.
Shang, A.H., Ye, J., Chen, D.H., Lu, X.X., Lu, H.D., Liu, C.N., Wang, L.M., 2015. Physiological effects of tetracycline antibiotic pollutants on non-target aquatic *Microcystis aeruginosa*. J. Environ. Sci. Health B 50 (11), 809–818. https://doi.org/10.1080/03601234.2015.1058100.
Sharma, L., Siedlewicz, G., Pazdro, K., 2021. The toxic effects of antibiotics on freshwater and marine photosynthetic microorganisms: state of the art. Plants 10 (3), 591. https://doi.org/10.3390/plants10030591.
Sharma, L., Kudłak, B., Siedlewicz, G., Pazdro, K., 2023. The effects of the IM1-12Br ionic liquid and the oxytetracycline mixture on selected marine and brackish microorganisms. Sci. Total Environ. 30 (901), 165898. https://doi.org/10.1016/j.scitotenv.2023.165898.
Siedlewicz, G., Białk-Bielińska, A., Borecka, M., Winogradow, A., Stepnowski, P., Pazdro, K., 2018. Presence, concentrations and risk assessment of selected antibiotic residues in sediments and near-bottom waters collected from the Polish coastal zone in the southern Baltic Sea - summary of 3 years of studies. Mar. Pollut. Bull. 129, 787–801. https://doi.org/10.1016/j.marpolbul.2017.10.075.
Siedlewicz, G., Żak, A., Sharma, L., Kosakowska, A., Pazdro, K., 2020. Effects of oxytetracycline on growth and chlorophyll *a* fluorescence in green algae (*Chlorella vulgaris*), diatom (*Phaeodactylum tricornutum*) and cyanobacteria (*Microcystis aeruginosa* and *Nodularia spumigena*). Oceanologia 62 (2), 214–225. https://doi.org/10.1016/j.oceano.2019.12.002.
Sobiechowska-Sasim, M., Stoń-Egiert, J., Kosakowska, A., 2014. Quantitative analysis of extracted phycobilin pigments in cyanobacteria an assessment of spectrophotometric and spectrofluorometric methods. J. Appl. Phycol. 26, 2065–2074. https://doi.org/10.1007/s10811-014-0244-3.
Sobotka, R., 2014. Making proteins green; biosynthesis of chlorophyll-binding proteins in cyanobacteria. Photosynth. Res. 119 (1–2), 223–232. https://doi.org/10.1007/s11120-013-9797-2.
Spindola, Vilela, C.L., Damasceno, T.L., Thomas, T., Peixoto, R.S., 2022. Global qualitative and quantitative distribution of micropollutants in the deep sea. Environ. Pollut. 15 (307), 119414. https://doi.org/10.1016/j.envpol.2022.119414.
Stadnichuk, I.N., Krasilnikov, P.M., Zlenko, D.V., 2015. Cyanobacterial phycobilisomes and phycobiliproteins. Microbiology 84, 101–111. https://doi.org/10.1134/S0026261715020150.
Stoń-Egiert, J., Kosakowska, A., 2005. RP-HPLC determination of phytoplankton pigments – comparison of calibration results for two columns. Mar. Biol. 147, 251–260. https://doi.org/10.1007/s00227-004-1551-z.
Strasser, R.J., Tsimilli-Michael, M., Srivastava, A., 2004. Analysis of the chlorophyll a fluorescence transient. In: Papageorgiou, G.C., Govindjee (Eds.), Chlorophyll a Fluorescence, Advances in Photosynthesis and Respiration, vol 19. Springer, Dordrecht. https://doi.org/10.1007/978-1-4020-3218-9_12.
Sydow, M., Owsianiak, M., Framski, G., Woźniak-Karczewska, M., Piotrowska-Cyplik, A., Ławniczak, Ł., Szulc, A., Zgoła-Grześkowiak, A., Heipieper, H.J., Chrzanowski, Ł., 2018. Biodiversity of soil bacteria exposed to sub-lethal concentrations of phosphonium-based ionic liquids: effects of toxicity and biodegradation. Ecotoxicol. Environ. Saf. 147, 157–164. https://doi.org/10.1016/j.ecoenv.2017.08.026.
Wada, N., Sakamoto, T., Matsugo, S., 2013. Multiple roles of photosynthetic and sunscreen pigments in cyanobacteria focusing on the oxidative stress. Metabolites 3 (2), 463–483. https://doi.org/10.3390/metabo3020463.
Wang, H., Wang, X., Jia, J., Qin, Y., Chen, S., Wang, S., Martyniuk, C.J., Yan, B., 2022. Comparative toxicity of [C8mim]Br and [C8py]Br in early developmental stages of zebrafish (*Danio rerio*) with focus on oxidative stress, apoptosis, and neurotoxicity. Environ. Toxicol. Pharmacol. 92, 103864. https://doi.org/10.1016/j.etap.2022.103864.
Wasmund, N., Dutz, J., Pollehne, F., Siegel, H., Zettler, M.L., 2016. Biological assessment of the Baltic Sea 2015. Meereswiss. Ber 102 (10.12754) doi:.io-warnemuende.de/10.12754/msr-2016-0102.
Wieczerzak, M., Kudłak, B., Namieśnik, J., 2016a. Study of the effect of residues of pharmaceuticals on the environment on the example of bioassay Microtox®. Monatsh. Chem. 147 (8), 1455–1460. https://doi.org/10.1007/s00706-016-1782-y.
Wieczerzak, M., Kudłak, B., Yotova, G., Nedyalkova, M., Tsakovski, S., Simeonov, V., Namieśnik, J., 2016b. Modeling of pharmaceuticals mixtures toxicity with deviation ratio and best-fit functions models. Sci. Total Environ. 571, 259–268. https://doi.org/10.1016/j.scitotenv.2016.07.186.
Xia, Y., Liu, D., Dong, Y., Chen, J., Liu, H., 2018. Effect of ionic liquids with different cations and anions on photosystem and cell structure of *Scenedesmus obliquus*. Chemosphere 195, 437–447. https://doi.org/10.1016/j.chemosphere.2017.12.054.
Zepernick, B.N., Niknejad, D.J., Stark, G.F., Truchon, A.R., Martin, R.M., Rossignol, K.L., Paerl, H.W., Wilhelm, S.W., 2022. Morphological, physiological, and transcriptional responses of the freshwater diatom *Fragilaria crotonensis* to elevated pH conditions. Front. Microbiol. 13, 1044464. https://doi.org/10.3389/fmicb.2022.1044464.